

Production and Decay of Neutralinos in the Next-To-Minimal Supersymmetric Standard Model

F. Franke*, H. Fraas

Institut für Theoretische Physik, Universität Würzburg
D-97074 Würzburg, Germany

Abstract

Within the framework of the Next-To-Minimal Supersymmetric Standard Model (NMSSM) we study neutralino production $e^+e^- \rightarrow \tilde{\chi}_i^0 \tilde{\chi}_j^0$ ($i, j = 1, \dots, 5$) at center-of-mass energies between 100 and 600 GeV and the decays of the heavier neutralinos into the LSP plus a fermion pair, a photon or a Higgs boson. For representative gaugino/higgsino mixing scenarios, where the light neutralinos have significant singlet components, we find some striking differences between the NMSSM and the minimal supersymmetric model. Since in the NMSSM neutralino and Higgs sector are strongly correlated, the decay of the second lightest neutralino into a Higgs boson and the LSP often is kinematically possible and even dominant in a large parameter region of typical NMSSM scenarios. Also, the decay rates into final states with a photon may be enhanced.

November 1995

* email: fabian@physik.uni-wuerzburg.de

1 Introduction

Supersymmetry (SUSY) [1] may provide a solution to the hierarchy and fine tuning problem of the standard model (SM) at the prize of more than doubling the particle spectrum [2]. Therefore the search for supersymmetric particles is one of the most challenging tasks at the present and future high energy colliders. The most popular supersymmetric extension of the SM is the Minimal Supersymmetric Standard Model (MSSM) [3] characterized by a minimal particle content and a minimal number of allowed couplings. In order to give mass to both up and down quarks and to avoid anomalies by higgsino loops, it contains two Higgs doublet fields H_1 and H_2 with hypercharge $\pm 1/2$ and vacuum expectation values v_1 and v_2 ($\tan \beta = v_2/v_1$). An essential feature of the MSSM is the conservation of a new quantum number called R -parity [4] that implies two important consequences: Supersymmetric particles can be produced only in pairs, and the lightest supersymmetric particle (LSP) is stable.

One of the most promising processes to detect a supersymmetric signature in e^+e^- collisions is the pair production of neutralinos, fermionic mass eigenstates composed of the supersymmetric partners of photon, Z boson and the neutral Higgs bosons. Since cosmological reasons suggest the lightest neutralino to be the LSP, at least one heavier neutralino must be produced which can be identified by its subsequent decays.

In the MSSM, LEP data imply a lower bound of 23 GeV for the lightest neutralino [5]. Neutralino production and decay has been discussed in great detail in refs. [6, 7] within the framework of the MSSM.

Many GUT and superstring theories [8, 9, 10], however, favor the minimal extension of the MSSM by a gauge singlet N with hypercharge 0, the *Next-To-Minimal Supersymmetric Standard Model* (NMSSM) [11, 12]. The most general superpotential of a supersymmetric model with an extra gauge singlet is

$$W = \lambda H_1 H_2 N - \mu H_1 H_2 - \frac{1}{3} k N^3 + \frac{1}{2} \mu' N^2 + \mu'' N, \quad (1)$$

which reduces to that of the MSSM if N is removed. In the NMSSM one considers only the trilinear terms

$$W_{\text{NMSSM}} = \lambda H_1 H_2 N - \frac{1}{3} k N^3, \quad (2)$$

so that the μ problem of the MSSM [13] is evaded. Recently it was claimed that cosmological implications of the NMSSM, namely the formation of domain walls at an early stage of the universe, require the Z_3 symmetry of the superpotential to be explicitly broken [14]. A solution to this domain wall problem would be the reintroduction of the μ term in the superpotential. Since an additional small μ term does not significantly affect the masses and mixings of the neutralinos but increases the number of free parameters we restrict ourselves to the superpotential of eq. (2).

Thus the basic difference between the MSSM and the NMSSM or other models with gauge singlets arise by the singlet components of neutralinos and Higgs bosons which do not couple to fermions, gauge bosons and their respective supersymmetric partners. In the NMSSM there are five neutralinos instead of four in the MSSM. Also the neutral Higgs sector is enlarged by one scalar and pseudoscalar Higgs bosons to three CP even

and two CP odd Higgs particles. As it was shown in refs. [15, 16], experimental data still allows for massless NMSSM neutralinos and Higgs bosons. We point out that these results do not change with the reintroduction of an additional μ term in the model, so that our choice of the superpotential eq. (2) instead of eq. (1) is well justified.

A further motivation for the NMSSM is the evasion of the usual MSSM Higgs mass bounds [17]. After including radiative corrections, the theoretical upper bound for the lightest Higgs scalar is increased by some 10 GeV compared to the MSSM [18].

Contrary to the minimal model, neutralino and Higgs sectors are strongly correlated in the NMSSM. The masses and mixings of neutralinos are given by the eigenvalues and eigenvectors of a 5×5 matrix that depends on the $SU(2)$ and $U(1)$ gaugino mass parameters M and M' , the singlet vacuum expectation value x , the ratio of the doublet expectation values $\tan \beta$ and the couplings λ and k in the superpotential. The properties of the neutral scalar and pseudoscalar Higgs bosons follow from two 3×3 matrices which at tree level contain the additional parameters A_λ and A_k of the soft symmetry breaking potential of the NMSSM

$$\begin{aligned}
V_{\text{soft}} = & m_1^2 |H_1|^2 + m_2^2 |H_2|^2 + m_3^2 |N|^2 \\
& + m_Q^2 |\tilde{Q}|^2 + m_{\tilde{U}}^2 |\tilde{U}|^2 + m_D^2 |\tilde{D}|^2 \\
& + m_L^2 |\tilde{L}|^2 + m_E^2 |\tilde{R}|^2 \\
& - (\lambda A_\lambda H_1 H_2 N + \text{h.c.}) - \left(\frac{1}{3} k A_k N^3 + \text{h.c.}\right) \\
& + (h_U A_U \tilde{Q} \tilde{U} H_2 - h_D A_D \tilde{Q} \tilde{D} H_1 - h_E A_E \tilde{L} \tilde{R} H_1 + \text{h.c.}) \\
& + \frac{1}{2} M \lambda^a \lambda^a + \frac{1}{2} M' \lambda' \lambda' .
\end{aligned} \tag{3}$$

In eq. (3) generation indices are suppressed and the notation of the $SU(2)$ doublet and $U(1)$ singlet fields is conventional.

The NMSSM offers an extremely interesting and complex variety of neutralino and Higgs phenomenology different from the minimal model [19, 20, 21, 22]. In this paper we analyze the production of neutralinos $e^+ e^- \rightarrow \tilde{\chi}_i^0 \tilde{\chi}_j^0$ ($i, j = 1, \dots, 5$) in the NMSSM. We focus on center-of-mass energies between 100 and 600 GeV, which cover the energy range of LEP2 up to that of a planned linear collider. In order to determine the supersymmetric signatures in the NMSSM we then discuss the subsequent neutralino decays into fermions, Higgs bosons and photons and compute the dominant decay channels in seven typical scenarios. For completeness we add an appendix with the neutralino and Higgs mixing matrices in the NMSSM and the relevant formulae for neutralino production and decay.

2 Scenarios

In this section we describe the seven scenarios A – G in which production and decay of neutralinos in the NMSSM are studied. They clearly differ from the MSSM by giving at least one of the light neutralinos a significant singlet component. Also we consider different values for the gaugino mass parameter M and the singlet vacuum expectation value x in order to cover various typical regions in the (M, x) -plane. Furthermore for

the decays of the NMSSM neutralinos the allowed mass regions for the light scalar and pseudoscalar Higgs bosons are of great importance. Since contrary to the MSSM the Higgs sector of the NMSSM is strongly correlated to the neutralino sector [16], the masses of the Higgs bosons are bounded already by fixing the parameters of the neutralino mass matrix.

Concerning the mass of the lightest neutralino which we assume to be the lightest supersymmetric particle (LSP) we choose on the one hand the scenarios A – D where the light neutralino has a mass of 10 GeV well below the mass bound for a MSSM neutralino, but we consider on the other hand also the scenarios E – G with a 50-GeV LSP. In order to demonstrate the differences between NMSSM and MSSM, in the first case the singlet component of the LSP $|\langle\chi_1^0|\psi_N\rangle|^2$ is larger than 90 %, while in the second case the second lightest neutralino has such a large singlet component $|\langle\chi_2^0|\psi_N\rangle|^2 > 0.9$. In all scenarios we restrict ourselves to a single value $\tan\beta = 2$.

Since we want to study the fundamental differences of neutralino production and decay in MSSM and NMSSM over a wide but for the NMSSM typical range of parameters we do not consider special solutions of the renormalization group equations of the NMSSM [23] as implied by supergravity models. Also we do not explicitly address the dark matter problem which has been studied in ref. [24] assuming the LSP to be the main component of dark matter.

First we present in Fig. 1 the parameter regions in the (λ, k) -plane of the trilinear couplings in the superpotential which lead to a very light or a singlet-like LSP. For three different values of the gaugino mass parameter $M = 65, 120, \text{ and } 200$ GeV, the contour lines for the mass $m_{\tilde{\chi}_1^0}$ of the lightest neutralino and its singlet component $|\langle\chi_1^0|\psi_N\rangle|^2$ are shown. Since only large singlet vacuum expectation values x allow for singlet components above 90 %, we set $x = 1000$ GeV. The experimentally excluded parameter space (for details see ref. [15]) is shaded. Note that the k axis ends at 0.1 since only for small couplings $k \lesssim 10^{-2}$ the mass of the LSP in the NMSSM can lie below the experimental bounds of the MSSM. For most of the (λ, k) -plane the LSP is heavier than 30 GeV. Larger masses for the LSP can be obtained with a broad range of k values, but for large couplings $k \gtrsim 0.1$ the coupling λ is limited to a narrow interval.

Generally, for smaller parameters M light neutralinos can exist in a larger region of the parameter space. The mass range approximately follows from the asymptotical values at large singlet vacuum expectation values x [25], $m_{\tilde{\chi}_i^0} \approx -\alpha M, -M, \lambda x, -\lambda x, -2kx$. Due to $m_{\tilde{\chi}_1^0} \lesssim \alpha M$ it is obvious that e. g. for $M = 65$ GeV and $x = 1000$ GeV a LSP with a mass as large as 50 GeV cannot exist.

Small couplings of the order $\mathcal{O}(10^{-2})$ are also necessary to obtain a large singlet component in the mixing of the lightest neutralino. The requirement of small couplings k for large singlet components is weakened for larger parameters M . While for $M = 200$ GeV a coupling $k \approx 0.3$ still leads to a singlet component $|\langle\psi_N|\chi_1^0\rangle|^2 > 0.9$, such a large singlet component is impossible with $M = 65$ GeV.

The scenarios A – D are constructed under the prerequisite that the lightest neutralino has a mass of about 10 GeV. For that we fix the couplings $\lambda = 0.4$ and $k = 0.001$ and keep in the scenarios A – C the parameters of Fig. 1: $\tan\beta = 2, x = 1000$ GeV, $M = 65, 120, 200$ GeV. With scenario D we want to study the consequences of a negative gaugino mass parameter $M = -120$ GeV. The masses and mixings of the neutralinos in these

scenarios are given in Tables 1 and 2. They mainly differ by the sign of the neutralino mass eigenvalues, the masses of the next lightest neutralinos and the chargino masses.

With the fixed values of λ , k , x and $\tan\beta$ and scanning over the parameters A_λ and A_k of the Higgs sector also the mass ranges for the scalar and pseudoscalar Higgs bosons and their mixings are identical in the scenarios A – D and shown in Table 3. Here also the experimental mass bounds as described in ref. [16] are included. Therefore, in our discussion of the neutralino decays in the scenarios A – D we may focus on the consequences of the different neutralino mass eigenvalues and mixings and can disregard variations of the Higgs masses. Because of this advantage we tolerate the slightly different masses of the LSP in these scenarios which, however, should not significantly alter the numerical results. The charged Higgs bosons are as heavy as 1 TeV in these scenarios and are therefore not relevant for the neutralino decays.

In the scenarios E – G (Tables 4 and 5) the lightest neutralino has a mass of 50 GeV. As it can be seen in Fig. 1, this mass value requires larger couplings k than in the scenarios A – D. Then also the singlet component of the LSP decreases, so that now the second lightest neutralino is mainly a singlet. Also in these scenarios with a heavier LSP we want to analyze the effect of the sign of the gaugino mass parameter M . In scenario E we first choose a positive value. But since negative gaugino mass parameters M allow for larger singlet components of the second lightest neutralino, the scenarios F and G are constructed with $M = -95$ GeV and $M = -90$ GeV, respectively, so that the differences to the MSSM are emphasized. While in scenarios E and F we retain the large singlet vacuum expectation value $x = 1000$ GeV with $\lambda = 0.4$, $k = 0.035$, $\tan\beta = 2$, we consider in scenario G a smaller singlet value $x = 300$ GeV and $\lambda = 0.4$, $k = 0.1$, $\tan\beta = 2$. This smaller x value leads to an increase of the doublet higgsino components of the light neutralinos and diminishes their zino components.

Also shown in Tables 4 and 5 is the allowed mass range for the scalar and pseudoscalar Higgs bosons scanning over the parameters A_λ and A_k of the Higgs sector. Since in both scenarios the mass differences between the light neutralinos is chosen to be rather small in order to enhance production cross sections even at LEP2 energies, the decay $\tilde{\chi}_2^0 \rightarrow \tilde{\chi}_1^0 + \text{Higgs}$ is kinematically not possible in scenarios E and F due to the large lower Higgs mass bound. We will discuss the neutralino decays in the NMSSM in detail later. Now we first focus on the neutralino production in the above described scenarios.

3 Production of NMSSM neutralinos

In this section we discuss the production of neutralinos at electron-positron colliders. Here we compute the cross sections for neutralino production in the seven scenarios and determine the center-of-mass energy necessary for the identification of a NMSSM neutralino. An analysis of the possible signatures from the decays follows in the next section.

Neutralino production $e^+e^- \rightarrow \tilde{\chi}_i^0\tilde{\chi}_j^0$ ($i, j = 1, \dots, 5$) proceeds via Z -exchange in the s channel and exchange of a selectron in the t and u channels. The corresponding Feynman graphs and the relevant eeZ , $\tilde{\chi}_i^0\tilde{\chi}_j^0Z$ and $e\tilde{e}\tilde{\chi}_i^0$ vertex factors are shown in Fig. 2. The notation is explained in the appendix where also the analytical formulae for the cross section are collected.

Since the singlet superfield has hypercharge 0, the singlet component of the neutralinos does not couple to (s)fermions and gauge bosons, so that the analytical expressions for neutralino production in the NMSSM are identical to those in the minimal model. The nevertheless often drastic differences merely arise by the mixings of the neutralinos. Before we analyze neutralino production in the previously presented scenarios we first want to make clear characteristic differences between MSSM and NMSSM with two simple examples. Let the MSSM be realized in the nature and imagine a MSSM scenario where only the LSP can be produced at a collider, e. g. LEP2, since the other neutralinos are too heavy. Then it would be impossible to detect a neutralino due to R-parity conservation. If, however, nature is described by the NMSSM, there could exist an additional light neutralino as LSP, so that the a neutralino with a similar mass but invisible in the MSSM could be identified by its decay into the LSP.

While in this example a NMSSM scenario could be verified more easily than the corresponding MSSM scenario, even the contrary could be possible: In the NMSSM the production of a singlet-like second lightest neutralinos could be heavily suppressed leading to two practically invisible neutralinos.

After this qualitative consideration we now come to the numerical results. Figs. 3 – 5 show the cross sections for neutralino production $e^+e^- \rightarrow \tilde{\chi}_i^0 \tilde{\chi}_j^0$ ($i, j = 1, \dots, 5$) as a function of the center-of-mass energy in the range $100 \text{ GeV} \leq \sqrt{s} \leq 600 \text{ GeV}$ covering the LEP2 energy $\sqrt{s} \approx 190 \text{ GeV}$ and the energy linear collider $\sqrt{s} = 500 \text{ GeV}$ of a future linear collider. Especially we want to determine the energy range where the cross sections in typical NMSSM scenarios reach magnitudes large enough in order to have reasonable chances for a detection.

All cross sections are computed with masses $m_{\tilde{e}_{L,R}} = 200 \text{ GeV}$ for the left-handed and right-handed selectron. This value lies well above the current mass bounds but is not so large that the production rates are heavily suppressed. We have neglected the mass splitting between left and right-handed selectrons as it appears within a unified theory [26], which, however, does not significantly alter the numerical results. The dependence of the cross sections on the selectron mass has already been studied in ref. [21]. For $m_{\tilde{e}_{L,R}} = 100 \text{ GeV}$ they increase by a factor of 2 – 5, for $m_{\tilde{e}_{L,R}} = 1000$ they decrease by one order of magnitude.

For the considered energy range above the Z -peak the cross sections are dominated by selectron exchange. Therefore the dependence on the center-of-mass energy is similar for all scenarios: After the kinematical threshold there begins a steep increase to the maximum which is followed by a flat decrease. The experimental identification of a neutralino may be facilitated in typical NMSSM scenarios with a light singlet-like LSP, where the next lightest neutralino is mainly composed of photinos and zinos. Since the selectron couple only to the photino/zino components of the neutralinos, this characteristic mixing type in our scenarios favors the production of the light neutralinos.

In scenario A the production of the three lightest neutralino is kinematically possible even for moderate collider energies and proceeds with cross sections above 10 fb in the channels $e^+e^- \rightarrow \tilde{\chi}_1^0 \tilde{\chi}_2^0, \tilde{\chi}_2^0 \tilde{\chi}_2^0, \tilde{\chi}_2^0 \tilde{\chi}_3^0, \tilde{\chi}_3^0 \tilde{\chi}_3^0$. The maximum lies around energies of 250 – 300 GeV but is approached already at the expected LEP2 energy of 190 GeV. For this energy the cross sections for pair production of the second and third lightest neutralino both reach 200 fb. In scenario A, the light chargino has a mass significantly below 100

GeV so that there are good chances to detect it at LEP2. Then pair production of $\tilde{\chi}_2^0$ followed by the decay into the LSP offers the possibility to discriminate between NMSSM and MSSM.

In scenario B with the larger gaugino mass parameter M , only the cross sections for $\tilde{\chi}_2^0\tilde{\chi}_2^0$ and $\tilde{\chi}_2^0\tilde{\chi}_3^0$ production are above 10 fb at $\sqrt{s} = 190$ GeV. For larger energies $\sqrt{s} \gtrsim 250$ GeV also pair production of $\tilde{\chi}_3^0$ reach values of about 100 fb. With increasing parameter M in scenario C finally only $\tilde{\chi}_1^0\tilde{\chi}_2^0$ production is kinematically possible at LEP2 energies but is heavily suppressed due to the strong singlet component of the LSP. This scenario makes clear, that a light NMSSM neutralino with mass of 10 GeV or below does not necessarily need to be detected at LEP2, while a 500-GeV linear collider definitely seems capable for verification or exclusion of a very light NMSSM neutralino provided that M is bounded by the fine-tuning or naturalness constraint

$$-400 \text{ GeV} \leq M \leq 400 \text{ GeV}. \quad (4)$$

This estimation arises by assuming a mass bound of about 1 TeV for all supersymmetric particles, especially the gluino, with

$$|M| = \frac{\alpha_2}{\alpha_3} m_{\tilde{g}} \simeq 0.3 m_{\tilde{g}}, \quad (5)$$

where the α_i are the gauge couplings of the symmetry groups.

Scenario D differs from scenario B mainly by the sign of the gaugino mass parameter and therefore by the relative signs of the mass eigenvalues of the light neutralinos. Further the singlet component of the LSP is slightly higher for negative M . Both lead to a decrease of the cross sections for production of the LSP together with another neutralino and an increase of the $\tilde{\chi}_2^0$ pair production due to the larger photino/zino component of the second lightest neutralino in scenario D compared to scenario B.

Since in the scenarios E – G the LSP already has a mass of 50 GeV, the production rates are rather low at LEP2 energies. While in scenario E the production of $\tilde{\chi}_2^0$ and $\tilde{\chi}_3^0$ together with the LSP proceeds at $\sqrt{s} = 190$ GeV with cross section above 10 fb, in scenarios F and G the cross sections for the production of the LSP with the third neutralino are around 100 fb. Here $\tilde{\chi}_1^0\tilde{\chi}_2^0$ production is favored in scenario E compared to the scenarios F and G because the singlet component of the second neutralino is reduced for positive parameters M , and the $\tilde{\chi}_1^0\tilde{\chi}_3^0$ production is suppressed due to the larger singlet component of the LSP. Even at higher energies the channels for neutralino detection are significantly reduced. Again only the third lightest neutralino is produced with rates of 100 fb in these scenarios, but in scenarios E and G also the second neutralino reaches cross section above 10 fb at high energies in the range of a linear collider.

Finally we consider in scenario G the case of smaller x values. While the neutralino production at $\sqrt{s} = 190$ GeV hardly differs from scenario E, this situation changes already at slightly higher energies $\sqrt{s} \gtrsim 200$ GeV: Now a variety of production channels opens, even the heavy neutralinos are produced with cross sections of about 30 – 50 fb. In such a scenario the interpretation of the experimental data and the verification of a concrete NMSSM scenario get rather complicated due to cascade decays of the heavy neutralinos.

The scenarios E – G show that the production of the singlet-like second lightest neutralino is heavily suppressed. Nevertheless the cross section at a future linear collider may

be sufficient for an identification by its subsequent decay into the LSP. Another possibility for a distinction of NMSSM and MSSM scenarios would be the decays of the heavier neutralinos into the singlet-like second neutralino. This is the subject of the next section.

4 Decay of NMSSM neutralinos

While the lightest neutralino as the LSP is stable and invisible in the MSSM as well as in the NMSSM, the other neutralino decay and can be detected in principle by their decay products. Since at the end of each decay chain the undetectable LSP is produced, missing energy is one essential supersymmetric signature. The heavy neutralinos can decay directly into the LSP, but also via numerous cascade decays. We restrict ourselves in this paper on the decays of the light neutralinos which are produced with a sufficiently large cross section. The following decays could represent the begin of a decay chain:

1. the decay of a heavy neutralino into a lighter one and two fermions $\tilde{\chi}_i^0 \longrightarrow \tilde{\chi}_j^0 e^+ e^-$, $\tilde{\chi}_j^0 \nu \bar{\nu}$, $\tilde{\chi}_j^0 q \bar{q}$ ($i > j$).

Since we assume these fermions to be massless, these decays are always kinematically allowed. They proceed via Z and sfermion exchange, their respective Feynman graphs are shown in Fig. 6 and the decay widths are given in the appendix. If one of the neutralinos has a large singlet component, the decay width for these three body decays gets rather small compared to the MSSM. We will emphasize this fact in the further discussion of the decays.

2. the decay of a heavy neutralino into a chargino and two fermions $\tilde{\chi}_i^0 \longrightarrow \tilde{\chi}_j^\pm e^\pm \nu$, $\tilde{\chi}_j^\pm q q'$.

In our scenarios the third neutralino is a few GeV heavier than the light chargino, so that this decay becomes kinematically possible. Due to the small mass difference it is, however, strongly suppressed compared to the three body decay into a light neutralino. Therefore we neglect this decay channel for the rest of this paper.

3. the decay of a heavy neutralino into a light neutralino and a photon $\tilde{\chi}_i^0 \longrightarrow \tilde{\chi}_j^0 \gamma$ ($i > j$).

This decay is always kinematically allowed. Since it proceeds in lowest order via a loop with W bosons, charginos and charged Higgs bosons or sfermions, it is suppressed compared to the tree level decays. The complete set of Feynman graphs can be found in ref. [27], we show in Fig. 6 only those with neutralino-chargino-Higgs couplings which differ from the MSSM.

Generally, the decay width of this loop decay is rather small. Therefore, in the MSSM it is relevant only if one of the neutralinos is nearly a pure photino and the other mainly a higgsino, so that the three body decay is also suppressed. In the NMSSM, however, both decay widths could be of the same order of magnitude. This is the case if one of the neutralinos has a large singlet component which explicitly affects the neutralino-chargino-Higgs coupling of the loop decay into a photon but just reduces the three body decay rates.

4. the decay of a heavy neutralino into a light neutralino and a scalar or pseudoscalar neutral Higgs boson $\tilde{\chi}_i^0 \rightarrow \tilde{\chi}_j^0 S_a, P_b$.

This decay proceeds at tree level via the Feynman graphs shown in Fig. 6 with the corresponding analytical formulae for the decay width given in the appendix. The Higgs-neutralino-neutralino coupling is significantly influenced by the singlet components of the neutralinos and the Higgs boson. In our scenarios with a light singlet-like neutralino there often exist also light neutral Higgs bosons, so that this decay becomes kinematically possible and dominant, while in the MSSM the actual Higgs mass bounds forbid such a light Higgs particle.

5. the decay of a heavy neutralino into a light neutralino or a chargino and a gauge boson, into a fermion and sfermion or into a chargino together with a charged Higgs boson.

Since in our scenarios the mass difference between the third neutralino and the LSP is maximal about 45 GeV, we do not consider these decays in the following.

If the decay $\tilde{\chi}_i^0 \rightarrow \tilde{\chi}_j^0 S_1/P_1$ dominates, the signatures of neutralino production crucially depend on the decay mechanism of the produced Higgs boson. Possible decay products are according to the masses and mixings two heavy quarks or leptons via $S_1/P_1 \rightarrow b\bar{b}, \tau\bar{\tau}$ or two neutralinos $S_1/P_1 \rightarrow \tilde{\chi}_1^0 \tilde{\chi}_1^0$. In the first case a clear signature may arise if the standard model background can be suppressed, in the second case the neutralino decay into the LSP plus a Higgs decay cannot be detected. Further, the channel $S_1 \rightarrow P_1 P_1$ could be the starting point for a cascade decay of the lightest Higgs scalar.

We now discuss the neutralino decays in our scenarios. First we consider in scenario A the decays of the second and third neutralino that can be produced at LEP2 or a linear collider. The branching ratios for these decays are depicted in Fig. 7 as a function of the mass of the light pseudoscalar Higgs boson. Since the lightest scalar Higgs boson has a mass of at least 37 GeV in the scenarios A – D, it can be produced only in the direct decay of the third neutralino into the LSP, then with branching ratios between 0 and 1 according to the choice of the parameters A_λ and A_k .

We show in Fig. 7 the maximal and minimal branching ratios scanning over all experimentally allowed values of A_λ and A_k . If the mass of the light pseudoscalar Higgs boson is smaller than the mass difference between the two lightest neutralinos, that is about 20 GeV in scenario A, the second lightest neutralino decays nearly completely into the LSP and P_1 . Then the signatures of $\tilde{\chi}_2^0$ depend on the dominant decay channels of the light pseudoscalar Higgs shown in Fig. 8. For pseudoscalar masses below 9 GeV the decay into a tau pair dominates. As soon as the decay into b quarks is kinematically possible, it contributes with at least 50 %. For $m_{P_1} > 16$ GeV also the invisible decay into two LSP takes place with a branching ratio up to 0.5.

If the pseudoscalar Higgs boson is heavier than 20 GeV, for the second neutralino the three body decays into two fermions and the LSP and the loop decay into one photon plus the LSP dominate. Their branching ratios are shown in Fig. 7 for one generation. Here the branching ratios of all decay channels are approximately of the same order, about 0.3 for each three body decay and up to 0.15 for the loop decay.

Since at least one neutral Higgs particle is lighter than the mass difference between the third neutralino and the LSP, the decay of $\tilde{\chi}_3^0$ into a Higgs boson and the LSP always dominates. Only if the masses of the scalar and pseudoscalar Higgs boson are near their upper bounds the other decay modes may contribute with a maximum of 60 %. The decay channels for the scalar Higgs boson in scenario A are $S_1 \rightarrow b\bar{b}, \tilde{\chi}_1^0\tilde{\chi}_1^0, P_1P_1$ with branching ratios shown in Fig. 9. The nearly complete decay into two pseudoscalars is possible, while for other Higgs parameters the invisible decay into two LSP may clearly dominate.

In scenario B the mass difference between the two lightest neutralinos becomes large enough to allow the decay of $\tilde{\chi}_2^0$ into a scalar Higgs boson. Therefore we show in Fig. 10 the branching ratios as a function of the mass of the lightest Higgs scalar. Again one sees the dominance of the neutralino decays into Higgs bosons. Only in a small Higgs mass range the other decays play some important role and reach branching ratios up to 50 %. Since the singlet component of the lightest neutralino increases from scenario A to scenario D, also the loop decay of the second neutralino into the LSP and a photon becomes more important.

Due to the large mass difference between the third lightest neutralino and the LSP in the scenarios B – D, the dominant $\tilde{\chi}_3^0$ decay mechanism always is the Higgs channel. Here the branching ratios are very similar to those of scenario A, with the possible subsequent Higgs decays into a pair of b quarks or two neutralinos according to the parameters A_λ and A_k of the Higgs sector. Therefore we discuss the $\tilde{\chi}_3^0$ decays not separately in every scenario B – D but refer to Figs. 7 – 9.

The scenarios E – G where the LSP has a mass of 50 GeV differ by the sign of the gaugino mass parameter M and the value of the singlet vacuum expectation value x . In these scenarios we do not take into consideration neutralino decays into Higgs bosons. As before these decays dominate if they are kinematically possible, then the produced Higgs boson decays dominantly into a b quark pair since the decay into two LSP is not possible due to their large mass. Instead we give in Table 6 numerical values for the decay widths and branching ratios for such parameters A_λ and A_k which do not allow neutralino decays into Higgs bosons. Concerning the decays of the singlet-like second lightest neutralino we now clearly see the differences between the scenarios. In scenario E with positive M and large x the leptonic three body decay dominates, while in scenario F with negative M and large x the loop decay into photons is dominant and in scenario G with negative M and smaller singlet vacuum expectation value x the hadronic three body decay is the most important. Due to the large singlet component of the second neutralino, the decay widths are always very small.

So the MSSM and the NMSSM can be clearly distinguished when a singlet-like visible neutralino is produced with cross sections large enough for detection. As discussed in the previous section, this is realized in scenarios E and G at a 500-GeV linear collider. The other possibility to verify a NMSSM scenario by the decays of the heavier neutralinos into the singlet-like second neutralino, however, seems to be locked. Table 6 shows that similar to the MSSM the direct decay of $\tilde{\chi}_3^0$ into the LSP dominates by far. The branching ratios for the significant NMSSM decay into the second neutralino can be neglected. This decay is strongly suppressed even in scenario E where the production of $\tilde{\chi}_2^0$, however, proceeds with sizable cross sections despite its large singlet component.

In order to estimate the full potential of neutralino search and to predict the chances for discriminating between NMSSM and MSSM at a particular future electron-positron collider, a detailed Monte-Carlo simulation of the SM background as well as of the supersymmetric processes has to be performed. Moreover, it should include a discussion of further relevant kinematical variables as missing momenta, angular and energy distribution. This goes well beyond the scope of this paper designed to demonstrate fundamental differences in the neutralino sector between the NMSSM and the minimal model .

5 Conclusion

Within the framework of the NMSSM, we analyzed production and decay of neutralinos in seven typical scenarios that are compatible with the experimental constraints from LEP and Tevatron. They differ by the values for the gaugino mass parameter M and for the singlet vacuum expectation value x . In four scenarios, the LSP is mainly a singlet with a mass of 10 GeV well below the current mass bound for a MSSM neutralino and therefore is mainly a singlet. In the other scenarios where now the second lightest neutralino has the largest singlet component the LSP has a mass of 50 GeV.

Typical cross sections for the production of singlet-like neutralinos at a 500-GeV electron-positron linear collider reach values between 10 and 100 fb. Even if the LSP is nearly massless, the next lightest neutralino can already be so heavy that no visible neutralino is produced at LEP2. Therefore, negative neutralino search at LEP2 is not expected to raise the lower neutralino mass bound in the NMSSM.

In scenarios with light, singlet-like neutralinos there often exist also light neutral Higgs bosons with masses below the MSSM bounds. In typical NMSSM scenarios, the neutralino decay into Higgs bosons may be dominant and allow for a discrimination between MSSM and NMSSM. In the parameter range where the decay into a Higgs boson and the LSP is kinematically forbidden, the loop decay into a photon and the LSP is enhanced compared to the three body decay into a fermion pair and the LSP, if the neutralinos have significant singlet components. For large singlet vacuum expectation values of about 1000 GeV, the loop decay may dominate with branching ratios up to 50 %.

If the lightest neutralino has a large singlet component, there are good chances for distinguishing MSSM and NMSSM since it is the last link of the decay chain and crucially determines the decay modes of the heavier neutralinos. If, however, the second lightest neutralino is mainly a singlet, the NMSSM can be verified only by its direct production and decay, since the decay cascades of the heavier neutralinos then omit the singlet-like neutralino.

Generally, neutralinos of the nonminimal model can manifest themselves in a variety of different signatures. Their identification can be facilitated by clear signatures with jets or photons in the final state. On the other hand, they could be invisible if they decay via Higgs bosons mainly into the LSP. In any case a careful analysis of the SM background and Monte-Carlo studies considering the detector efficiency are indispensable for the verification of minimal or nonminimal supersymmetry.

Acknowledgements

The authors would like to thank A. Bartl for many helpful discussions. Support by the Deutsche Forschungsgemeinschaft under contract no. FR 1064/2-1 is gratefully acknowledged.

Appendix

A Neutralino mixing

The neutralino mass terms are contained in the following part of the NMSSM Lagrangian

$$\begin{aligned}
\mathcal{L} = & \frac{1}{\sqrt{2}}ig\lambda^3(v_1\psi_{H_1}^1 - v_2\psi_{H_2}^2) - \frac{1}{\sqrt{2}}ig'\lambda'(v_1\psi_{H_1}^1 - v_2\psi_{H_2}^2) \\
& - \frac{1}{2}M\lambda^3\lambda^3 - \frac{1}{2}M'\lambda'\lambda' \\
& - \lambda x\psi_{H_1}^1\psi_{H_2}^2 - \lambda v_1\psi_{H_2}^2\psi_N - \lambda v_2\psi_{H_1}^1\psi_N + kx\psi_N^2 \\
& + \text{h.c.}
\end{aligned} \tag{6}$$

where λ^3 , λ' , $\psi_{H_1}^1$ and $\psi_{H_2}^2$ are the two component spinors of the supersymmetric partners of the neutral gauge and Higgs bosons. As a basis of the neutral gaugino-higgsino system we take

$$(\psi^0)^T = (-i\lambda_\gamma, -i\lambda_Z, \psi_H^a, \psi_H^b, \psi_N) \tag{7}$$

with the higgsino states

$$\begin{aligned}
\psi_H^a &= \psi_{H_1}^1 \cos \beta - \psi_{H_2}^2 \sin \beta \\
\psi_H^b &= \psi_{H_1}^1 \sin \beta + \psi_{H_2}^2 \cos \beta.
\end{aligned} \tag{8}$$

Then the mass term reads

$$\mathcal{L} = -\frac{1}{2}(\psi^0)^T Y \psi^0 + \text{h.c.} \tag{9}$$

with the neutralino mass matrix

$$Y = \begin{pmatrix} -Ms_W^2 - M'c_W^2 & (M' - M)s_Wc_W & 0 & 0 & 0 \\ (M' - M)s_Wc_W & -Mc_W^2 - M's_W^2 & m_Z & 0 & 0 \\ 0 & m_Z & -\lambda x \sin 2\beta & \lambda x \cos 2\beta & 0 \\ 0 & 0 & \lambda x \cos 2\beta & \lambda x \sin 2\beta & \lambda v \\ 0 & 0 & 0 & \lambda v & -2kx \end{pmatrix}. \tag{10}$$

Here we introduced the abbreviations

$$s_W \equiv \sin \theta_W, \quad c_W \equiv \cos \theta_W, \quad v \equiv \sqrt{v_1^2 + v_2^2}. \tag{11}$$

In this paper we employ the usual gaugino mass relation

$$M' = \frac{5}{3} \frac{g_1}{g_2} M \simeq 0.5M, \tag{12}$$

with the couplings g_i of the $U(1)$ and $SU(2)$ gauge groups.

In the limit $\lambda, k \rightarrow 0$ with λx and kx fixed the neutralino mass matrix decouples, and the upper 4×4 matrix corresponds to that of the MSSM with $\mu = \lambda x$ [28].

The neutralino mass matrix can be diagonalized by a unitary 5×5 matrix N

$$m_{\tilde{\chi}_i^0} \delta_{ij} = N_{im}^* Y_{mn} N_{jn}, \quad (13)$$

where the $m_{\tilde{\chi}_i^0}$ are the mass eigenvalues of the neutralino states

$$\chi_i^0 = N_{ij} \psi_j^0 \quad i, j = 1, \dots, 5. \quad (14)$$

Finally, one obtains the proper four-component neutralino mass eigenstates by defining the Majorana spinors

$$\tilde{\chi}_i^0 = \begin{pmatrix} \chi_i^0 \\ \bar{\chi}_i^0 \end{pmatrix} \quad i, j = 1, \dots, 5. \quad (15)$$

B Higgs mixing

Here we present the most important results for the Higgs sector. Including radiative corrections from top and stop loops the mass squared matrix for the neutral scalar Higgs bosons reads [18]

$$\mathcal{M}_S^2 = \begin{pmatrix} M_{11}^{S^2} & M_{12}^{S^2} & M_{13}^{S^2} \\ M_{12}^{S^2} & M_{22}^{S^2} & M_{23}^{S^2} \\ M_{13}^{S^2} & M_{23}^{S^2} & M_{33}^{S^2} \end{pmatrix} + \delta \mathcal{M}_S^2 \quad (16)$$

with the matrix elements at tree level

$$M_{11}^{S^2} = \frac{(g^2 + g'^2)v_1^2}{2} + \lambda x(A_\lambda + kx) \tan \beta, \quad (17)$$

$$M_{12}^{S^2} = \frac{v_1 v_2}{2} (4\lambda^2 - g^2 - g'^2) - \lambda x(A_\lambda + kx), \quad (18)$$

$$M_{13}^{S^2} = 2\lambda^2 v_1 x - 2\lambda k x v_2 - \lambda A_\lambda v_2, \quad (19)$$

$$M_{22}^{S^2} = \frac{(g^2 + g'^2)v_2^2}{2} + \lambda x(A_\lambda + kx) \cot \beta, \quad (20)$$

$$M_{23}^{S^2} = 2\lambda^2 v_2 x - 2\lambda k x v_1 - \lambda A_\lambda v_1, \quad (21)$$

$$M_{33}^{S^2} = 4k^2 x^2 - k A_k x + \frac{\lambda A_\lambda v_1 v_2}{x}, \quad (22)$$

and the radiative corrections

$$\delta \mathcal{M}_S^2 = \begin{pmatrix} \Delta_{11}^2 & \Delta_{12}^2 & \Delta_{13}^2 \\ \Delta_{12}^2 & \Delta_{22}^2 & \Delta_{23}^2 \\ \Delta_{13}^2 & \Delta_{23}^2 & \Delta_{33}^2 \end{pmatrix} + \begin{pmatrix} \tan \beta & -1 & -\frac{v_2}{x} \\ -1 & \cot \beta & -\frac{v_1}{x} \\ -\frac{v_2}{x} & -\frac{v_1}{x} & \frac{v_1 v_2}{x^2} \end{pmatrix} \Delta^2 \quad (23)$$

with

$$\Delta^2 = \frac{3}{16\pi^2} h_t^2 \lambda x A_t f(m_{\tilde{t}_1}^2, m_{\tilde{t}_2}^2), \quad (24)$$

$$\Delta_{11}^2 = \frac{3}{8\pi^2} h_t^4 v_2^2 \lambda^2 x^2 \left(\frac{A_t + \lambda x \cot \beta}{m_{\tilde{t}_2}^2 - m_{\tilde{t}_1}^2} \right)^2 g(m_{\tilde{t}_1}^2, m_{\tilde{t}_2}^2), \quad (25)$$

$$\begin{aligned} \Delta_{12}^2 &= \frac{3}{8\pi^2} h_t^4 v_2^2 \lambda x \left(\frac{A_t + \lambda x \cot \beta}{m_{\tilde{t}_2}^2 - m_{\tilde{t}_1}^2} \right) \\ &\times \left(\log \left(\frac{m_{\tilde{t}_2}^2}{m_{\tilde{t}_1}^2} \right) + \frac{A_t(A_t + \lambda x \cot \beta)}{m_{\tilde{t}_2}^2 - m_{\tilde{t}_1}^2} g(m_{\tilde{t}_1}^2, m_{\tilde{t}_2}^2) \right), \end{aligned} \quad (26)$$

$$\begin{aligned} \Delta_{13}^2 &= \frac{3}{8\pi^2} h_t^4 v_2^2 \lambda^2 v_1 x \left(\frac{A_t + \lambda x \cot \beta}{m_{\tilde{t}_2}^2 - m_{\tilde{t}_1}^2} \right)^2 g(m_{\tilde{t}_1}^2, m_{\tilde{t}_2}^2) \\ &- \frac{3}{8\pi^2} h_t^4 \lambda^2 v_1 x f(m_{\tilde{t}_1}^2, m_{\tilde{t}_2}^2), \end{aligned} \quad (27)$$

$$\begin{aligned} \Delta_{22}^2 &= \frac{3}{8\pi^2} h_t^4 v_2^2 \left(\log \left(\frac{m_{\tilde{t}_1}^2 m_{\tilde{t}_2}^2}{m_t^4} \right) + \frac{2A_t(A_t + \lambda x \cot \beta)}{m_{\tilde{t}_2}^2 - m_{\tilde{t}_1}^2} \log \left(\frac{m_{\tilde{t}_2}^2}{m_{\tilde{t}_1}^2} \right) \right) \\ &+ \frac{3}{8\pi^2} h_t^4 v_2^2 \left(\frac{A_t(A_t + \lambda x \cot \beta)}{m_{\tilde{t}_2}^2 - m_{\tilde{t}_1}^2} \right)^2 g(m_{\tilde{t}_1}^2, m_{\tilde{t}_2}^2), \end{aligned} \quad (28)$$

$$\begin{aligned} \Delta_{23}^2 &= \frac{3}{8\pi^2} h_t^4 v_2^2 \lambda v_1 \left(\frac{A_t + \lambda x \cot \beta}{m_{\tilde{t}_2}^2 - m_{\tilde{t}_1}^2} \right) \\ &\times \left(\log \left(\frac{m_{\tilde{t}_2}^2}{m_{\tilde{t}_1}^2} \right) + \frac{A_t(A_t + \lambda x \cot \beta)}{m_{\tilde{t}_2}^2 - m_{\tilde{t}_1}^2} g(m_{\tilde{t}_1}^2, m_{\tilde{t}_2}^2) \right), \end{aligned} \quad (29)$$

$$\Delta_{33}^2 = \frac{3}{8\pi^2} h_t^4 v_2^2 \lambda^2 v_1^2 \left(\frac{A_t + \lambda x \cot \beta}{m_{\tilde{t}_2}^2 - m_{\tilde{t}_1}^2} \right)^2 g(m_{\tilde{t}_1}^2, m_{\tilde{t}_2}^2). \quad (30)$$

Here $m_{\tilde{t}_1}$ and $m_{\tilde{t}_2}$ are the stop masses, A_t is the mass parameter in the soft symmetry breaking potential eq. (3) connected with the top quark. The functions f and g are defined as

$$f(m_{\tilde{t}_1}^2, m_{\tilde{t}_2}^2) = \frac{1}{m_{\tilde{t}_2}^2 - m_{\tilde{t}_1}^2} \left(m_{\tilde{t}_1}^2 \log \left(\frac{m_{\tilde{t}_1}^2}{\mu^2} \right) - m_{\tilde{t}_2}^2 \log \left(\frac{m_{\tilde{t}_2}^2}{\mu^2} \right) - m_{\tilde{t}_1}^2 + m_{\tilde{t}_2}^2 \right), \quad (31)$$

$$g(m_{\tilde{t}_1}^2, m_{\tilde{t}_2}^2) = \frac{-1}{m_{\tilde{t}_2}^2 - m_{\tilde{t}_1}^2} \left((m_{\tilde{t}_1}^2 + m_{\tilde{t}_2}^2) \log \left(\frac{m_{\tilde{t}_2}^2}{m_{\tilde{t}_1}^2} \right) + 2(m_{\tilde{t}_1}^2 - m_{\tilde{t}_2}^2) \right) \quad (32)$$

with the $\overline{\text{MS}}$ renormalization scale μ .

For the pseudoscalar Higgs bosons one obtains the mass squared matrix

$$\mathcal{M}_P^2 = \begin{pmatrix} M_{11}^{P^2} & M_{12}^{P^2} & M_{13}^{P^2} \\ M_{12}^{P^2} & M_{22}^{P^2} & M_{23}^{P^2} \\ M_{13}^{P^2} & M_{23}^{P^2} & M_{33}^{P^2} \end{pmatrix} + \delta \mathcal{M}_P^2, \quad (33)$$

where the tree level matrix elements are

$$M_{11}^{P^2} = \lambda x (A_\lambda + kx) \tan \beta, \quad (34)$$

$$M_{12}^{P^2} = \lambda x (A_\lambda + kx), \quad (35)$$

$$M_{13}^{P^2} = \lambda v_2 (A_\lambda - 2kx), \quad (36)$$

$$M_{22}^{P^2} = \lambda x (A_\lambda + kx) \cot \beta, \quad (37)$$

$$M_{23}^{P^2} = \lambda v_1 (A_\lambda - 2kx), \quad (38)$$

$$M_{33}^{P^2} = \lambda A_\lambda \frac{v_1 v_2}{x} + 4\lambda k v_1 v_2 + 3k A_k x, \quad (39)$$

and the radiative corrections can be written as

$$\delta \mathcal{M}_P^2 = \begin{pmatrix} \tan \beta & 1 & \frac{v_2}{x} \\ 1 & \cot \beta & \frac{v_1}{x} \\ \frac{v_2}{x} & \frac{v_1}{x} & \frac{v_1 v_2}{x^2} \end{pmatrix} \Delta^2. \quad (40)$$

One eigenvalue of the mass matrix for the pseudoscalar Higgs bosons corresponds to an unphysical massless Goldstone mode.

The mass eigenstates of the scalar Higgs bosons are denoted by S_i ($i = 1, 2, 3$), ($m_{S_1} \leq m_{S_2} \leq m_{S_3}$) and those of the physical pseudoscalars by P_j ($j = 1, 2$), ($m_{P_1} \leq m_{P_2}$). They follow from the Higgs fields H_1^0 , H_2^0 and N by transformation with the diagonalization matrices U^S and U^P

$$\begin{pmatrix} S_1 \\ S_2 \\ S_3 \end{pmatrix} = \sqrt{2} U^S \left[\begin{pmatrix} \text{Re} H_1^0 \\ \text{Re} H_2^0 \\ \text{Re} N \end{pmatrix} - \begin{pmatrix} v_1 \\ v_2 \\ x \end{pmatrix} \right], \quad (41)$$

$$\begin{pmatrix} P_1 \\ P_2 \end{pmatrix} = \sqrt{2} U^P \begin{pmatrix} \text{Im} H_1^0 \\ \text{Im} H_2^0 \\ \text{Im} N \end{pmatrix}. \quad (42)$$

Since we omit the unphysical Goldstone bosons, U^P is a 3×2 matrix transforming the imaginary parts of the Higgs fields in the Lagrangian to the physical pseudoscalar Higgs bosons.

C Cross sections and decay widths

For the analytical formulae for neutralino production and decay we use the following notation:

1. the parameters in the couplings between a Z boson and two fermions are

$$L_f = T_{3f} - e_f \sin^2 \theta_W, \quad R_f = -e_f \sin^2 \theta_W, \quad (43)$$

where e_f and T_{3f} denote the charge and the isospin of the fermion, respectively;

2. the parameters in the coupling between a Z boson and two neutralinos are

$$O_{ij}^{\prime\prime L} = -\frac{1}{2} (N_{i3} N_{j3}^* - N_{i4} N_{j4}^*) \cos 2\beta - \frac{1}{2} (N_{i3} N_{j4}^* - N_{i4} N_{j3}^*) \sin 2\beta, \quad (44)$$

$$O_{ij}^{\prime\prime R} = -O_{ij}^{\prime\prime L*}, \quad (45)$$

where N_{ij} denote the mixing components of the neutralinos in the basis (7);

3. the parameters in the couplings between a scalar Higgs boson and two neutralinos are

$$\begin{aligned}
Q_{aij}^{L''} = & \frac{1}{2} \left[(U_{a1}^S \cos \beta + U_{a2}^S \sin \beta) \left(\frac{g}{c_W} (N_{i2} N_{j3}^* + N_{j2} N_{i3}^*) \right. \right. \\
& + \sqrt{2} \lambda (N_{i5} N_{j4}^* + N_{j5} N_{i4}^*) \\
& + (U_{a1}^S \sin \beta - U_{a2}^S \cos \beta) \left(\frac{g}{c_W} (N_{i2} N_{j4}^* + N_{j2} N_{i4}^*) \right. \\
& \left. \left. - \sqrt{2} \lambda (N_{i5} N_{j3}^* + N_{j5} N_{i3}^*) \right) \right] \\
& - \sqrt{2} k U_{a3}^S (N_{i5} N_{j5}^* + N_{j5} N_{i5}^*), \tag{46}
\end{aligned}$$

$$Q_{aij}^{R''} = Q_{aij}^{L''*}, \tag{47}$$

where U^S is the diagonalization matrix of the scalar Higgs sector in eq. (41);

4. the parameters in the couplings between a pseudoscalar Higgs boson and two neutralinos are

$$\begin{aligned}
R_{\alpha ij}^{L''} = & -\frac{1}{2} \left[(U_{\alpha 1}^P \cos \beta + U_{\alpha 2}^P \sin \beta) \left(\frac{g}{c_W} (N_{i2} N_{j3}^* + N_{j2} N_{i3}^*) \right. \right. \\
& - \sqrt{2} \lambda (N_{i5} N_{j4}^* + N_{j5} N_{i4}^*) \\
& + (U_{\alpha 1}^P \sin \beta - U_{\alpha 2}^P \cos \beta) \left(\frac{g}{c_W} (N_{i2} N_{j4}^* + N_{j2} N_{i4}^*) \right. \\
& \left. \left. + \sqrt{2} \lambda (N_{i5} N_{j3}^* + N_{j5} N_{i3}^*) \right) \right], \\
& - \sqrt{2} k U_{\alpha 3}^P (N_{i5} N_{j5}^* + N_{j5} N_{i5}^*) \tag{48}
\end{aligned}$$

$$R_{\alpha ij}^{R''} = -R_{\alpha ij}^{L''*}, \tag{49}$$

where U^P is the diagonalization matrix of the pseudoscalar Higgs sector in eq. (42);

5. the parameters in the coupling between a neutralino, a scalar lepton or scalar quark and a lepton or quark are

$$f_{fi}^L = -\sqrt{2} \left[\frac{1}{\cos \theta_W} L_f N_{i2} - \frac{1}{\sin \theta_W} R_f N_{i1} \right] \tag{50}$$

$$f_{fi}^R = -\sqrt{2} e_f \sin \theta_W [\tan \theta_W N_{i2}^* - N_{i1}^*]; \tag{51}$$

6. the Z propagator

$$D_Z(x) = (x - m_Z^2 + im_Z \Gamma_Z)^{-1}; \tag{52}$$

7. the triangle function

$$\lambda(a, b, c) = a^2 + b^2 + c^2 - 2ab - 2ac - 2bc. \tag{53}$$

Then one finds for the cross sections of the process $e^+e^- \rightarrow \tilde{\chi}_i^0 \tilde{\chi}_j^0$ [6]

$$\sigma_{\text{tot}} = \frac{1}{2} (\sigma_Z + \sigma_{\tilde{e}} + \sigma_{Z\tilde{e}}) (2 - \delta_{ij}). \quad (54)$$

The particular terms arise from Z and selectron exchange and their interference

$$\sigma_Z = \frac{g^4}{4\pi \cos^4 \theta_W} |D_Z(s)|^2 \frac{q}{\sqrt{s}} |O_{ij}''^L|^2 (|L_e|^2 + |R_e|^2) \left[E_i E_j + \frac{1}{3} q^2 - m_i m_j \right], \quad (55)$$

$$\begin{aligned} \sigma_{\tilde{e}} = & \frac{g^4}{16\pi s \sqrt{s}} \left\{ |f_{ei}^L|^2 |f_{ej}^L|^2 \left[\frac{E_i E_j - s d_L + q^2}{s d_L - q^2} + 2 + \frac{\sqrt{s}}{2q} \left(1 - 2d_L - \frac{m_i m_j}{s d_L} \right) \right. \right. \\ & \left. \left. \times \ln \left| \frac{d_L + q/\sqrt{s}}{d_L - q/\sqrt{s}} \right| \right] + (L \leftrightarrow R) \right\}, \quad (56) \end{aligned}$$

$$\begin{aligned} \sigma_{Z\tilde{e}} = & -\frac{g^4}{8\pi \cos^2 \theta_W} \frac{q}{\sqrt{s}} \text{Re} (D_Z(s)) O_{ij}''^L \\ & \times \left\{ L_e f_{ei}^L f_{ej}^L \left[\frac{1}{q\sqrt{s}} (E_i E_j - s d_L (1 - d_L) - m_i m_j) \ln \left| \frac{d_L + q/\sqrt{s}}{d_L - q/\sqrt{s}} \right| + 2(1 - d_L) \right] \right. \\ & \left. - (L \leftrightarrow R) \right\} \quad (57) \end{aligned}$$

with

$$d_{L,R} = \frac{1}{2s} (s + 2m_{\tilde{e}_{L,R}}^2 - m_i^2 - m_j^2). \quad (58)$$

Here, q is the momentum of $\tilde{\chi}_i^0$ in the e^+e^- center-of-mass system

$$q = \frac{1}{2\sqrt{s}} \sqrt{\lambda(s, m_i^2, m_j^2)}, \quad (59)$$

and $E_i = \sqrt{q^2 + m_i^2}$.

The decay width for the three body decay of a neutralino as shown in Fig. 6 can be written as

$$\Gamma(\tilde{\chi}_i^0 \rightarrow \tilde{\chi}_j^0 + f + \bar{f}) = N_c \frac{g^4}{(2\pi)^3 64 |m_i|^3} \int d\bar{s} d\bar{t} (W_s + W_t + W_u + W_{tu} + W_{st} + W_{su}) \quad (60)$$

with

$$\begin{aligned} W_s = & |D_Z(\bar{s})|^2 \frac{4|O_{ij}''^L|^2 (L_f^2 + R_f^2)}{\cos^4 \theta_W} \\ & \times \left[(m_i^2 - \bar{t})(\bar{t} - m_j^2) + (m_i^2 - \bar{u})(\bar{u} - m_j^2) + 2m_i m_j \bar{s} \right], \quad (61) \end{aligned}$$

$$W_t = |f_{fi}^L|^2 |f_{fj}^L|^2 \frac{(m_i^2 - \bar{t})(\bar{t} - m_j^2)}{(\bar{t} - m_{f_L}^2)^2} + (L \leftrightarrow R), \quad (62)$$

$$W_u = W_t(\bar{t} \leftrightarrow \bar{u}), \quad (63)$$

$$W_{tu} = |f_{fi}^L|^2 |f_{fj}^L|^2 \frac{2m_i m_j \bar{s}}{(\bar{t} - m_{f_L}^2)(\bar{u} - m_{f_L}^2)} + (L \leftrightarrow R), \quad (64)$$

$$W_{st} = \frac{4\text{Re}(D_Z(\bar{s}))}{(\bar{t} - m_{\tilde{f}_L}^2)} \frac{f_{fi}^L f_{fj}^L O_{ij}^{\prime\prime L} L_f}{\cos^2 \theta_W} \times \left[(m_i^2 - \bar{t})(\bar{t} - m_j^2) + m_i m_j \bar{s} \right] + (L \leftrightarrow R), \quad (65)$$

$$W_{su} = W_{st}(\bar{t} \leftrightarrow \bar{u}). \quad (66)$$

Here the integration bounds are $\bar{s}_{\min} = 0$, $\bar{s}_{\max} = (|m_i| - |m_j|)^2$, $\bar{t}_{\max, \min} = \frac{1}{2} (m_i^2 + m_j^2 - \bar{s} \pm \sqrt{\lambda(m_i^2, m_j^2, \bar{s})})$, and $\bar{u} = m_i^2 + m_j^2 - \bar{s} - \bar{t}$. The factor N_c has the value 1 for the decay into leptons and 3 for the decay into a quark pair.

Further we computed in this paper the decay width for the loop decay into a lighter neutralino and a photon. Due to its lengthy structure we do not state the analytical formula. It can be found in ref. [27] for the MSSM, for the NMSSM one has to replace the parameters $Q_{ij}^{\prime L}$ and $Q_{ij}^{\prime R}$ in the $\tilde{\chi}^0 \tilde{\chi}^\pm H^\mp$ couplings by

$$Q_{ij}^{\prime L} = g \cos \beta \left[(-N_{i3} \sin \beta + N_{i4} \cos \beta) V_{j1} + \frac{1}{\sqrt{2}} \left(2s_W N_{i1} + (c_W - \frac{s_W^2}{c_W}) N_{i2} \right) V_{j2} \right] - \lambda^* \sin \beta N_{i5} V_{j2}, \quad (67)$$

$$Q_{ij}^{\prime R} = g \sin \beta \left[(N_{i3} \cos \beta + N_{i4} \sin \beta) U_{j1} - \frac{1}{\sqrt{2}} \left(2s_W N_{i1} + (c_W - \frac{s_W^2}{c_W}) N_{i2} \right) U_{j2} \right] - \lambda^* \cos \beta N_{i5} U_{j2}. \quad (68)$$

For details of the NMSSM couplings see ref. [29].

The decay widths for the neutralino decay into a lighter neutralino and a neutral scalar or pseudoscalar Higgs boson read

$$\Gamma(\tilde{\chi}_i^0 \rightarrow \tilde{\chi}_j^0 + S_a) = \frac{\sqrt{\lambda(m_i^2, m_j^2, m_a^2)}}{16\pi|m_i|^3} Q_{aij}^{\prime\prime L^2} \left[(m_i^2 + m_j^2 - m_a^2) + 2m_i m_j \right], \quad (69)$$

$$\Gamma(\tilde{\chi}_i^0 \rightarrow \tilde{\chi}_j^0 + P_\alpha) = \frac{\sqrt{\lambda(m_i^2, m_j^2, m_\alpha^2)}}{16\pi|m_i|^3} R_{\alpha ij}^{\prime\prime L^2} \left[(m_i^2 + m_j^2 - m_\alpha^2) - 2m_i m_j \right]. \quad (70)$$

For the subsequent decays of the produced light Higgs bosons one obtains the following decay widths for

1. the decay of a scalar Higgs boson into a pair of up type fermions

$$\Gamma(S_a \rightarrow f\bar{f}) = N_c \frac{g^2 m_f^2}{32\pi m_W^2 \sin^2 \beta} m_a U_{a2}^S \left(1 - \frac{4m_f^2}{m_a^2} \right)^{3/2}; \quad (71)$$

2. the decay of a scalar Higgs boson into a pair of down type fermions

$$\Gamma(S_a \rightarrow f\bar{f}) = N_c \frac{g^2 m_f^2}{32\pi m_W^2 \cos^2 \beta} m_a U_{a1}^S \left(1 - \frac{4m_f^2}{m_a^2} \right)^{3/2}; \quad (72)$$

3. the decay of a pseudoscalar Higgs boson into a pair of up type fermions

$$\Gamma(P_\alpha \rightarrow f\bar{f}) = N_c \frac{g^2 m_f^2}{32\pi m_W^2 \sin^2 \beta} m_\alpha U_{\alpha 2}^{P^2} \left(1 - \frac{4m_f^2}{m_a^2}\right)^{1/2}; \quad (73)$$

4. the decay of a pseudoscalar Higgs boson into a pair of down type fermions

$$\Gamma(P_\alpha \rightarrow f\bar{f}) = N_c \frac{g^2 m_f^2}{32\pi m_W^2 \cos^2 \beta} m_\alpha U_{\alpha 1}^{P^2} \left(1 - \frac{4m_f^2}{m_a^2}\right)^{1/2}; \quad (74)$$

5. the decay of a scalar or pseudoscalar Higgs boson into two neutralinos

$$\Gamma(S_a \rightarrow \tilde{\chi}_i^0 \tilde{\chi}_j^0) = \frac{\sqrt{\lambda(m_a^2, m_i^2, m_j^2)}}{8\pi m_a^3 (1 + \delta_{ij})} Q_{\alpha ij}^{\prime\prime L^2} [(m_a^2 - m_i^2 - m_j^2) - 2m_i m_j], \quad (75)$$

$$\Gamma(P_\alpha \rightarrow \tilde{\chi}_i^0 \tilde{\chi}_j^0) = \frac{\sqrt{\lambda(m_\alpha^2, m_i^2, m_j^2)}}{8\pi m_\alpha^3 (1 + \delta_{ij})} R_{\alpha ij}^{\prime\prime L^2} [(m_\alpha^2 - m_i^2 - m_j^2) + 2m_i m_j]; \quad (76)$$

6. the decay of a scalar Higgs boson into two light pseudoscalar Higgs particles

$$\Gamma(S_a \rightarrow P_\beta P_\gamma) = \frac{\sqrt{\lambda(m_a^2, m_\beta^2, m_\gamma^2)}}{16\pi m_a^3 (1 + \delta_{\beta\gamma})} g_{S_a P_\beta P_\gamma}^2. \quad (77)$$

The couplings $g_{S_a P_\beta P_\gamma}$ between one scalar and two pseudoscalar Higgs bosons can be found in ref. [29].

References

- [1] Y.A. Goldfand and E.P. Likhtman, JETP Lett. **13** (1971) 323;
D.V. Volkov and V.P. Akulov, Phys. Lett. **B 46** (1974) 39;
J. Wess and B. Zumino, Nucl. Phys. **B 70** (1974) 39; Phys. Lett. **B 49** (1974) 52;
Nucl. Phys. **B 78** (1974) 1
- [2] For reviews, see e. g. P. Fayet and S. Ferrara, Phys. Rep. **32** (1977) 249;
H.P. Nilles, Phys. Rep. **110** (1984) 1
- [3] H.E. Haber and G.L. Kane, Phys. Rep. **117** (1985) 75
- [4] P. Fayet, Phys. Lett. **B 69** (1977) 489;
G. Farrar and P. Fayet, Phys. Lett. **B 76** (1978) 575
- [5] L3 Collaboration, M. Acciarri et al., Phys. Lett. **B 350** (1995) 109
- [6] A. Bartl, H. Fraas and W. Majerotto, Nucl. Phys. **B 278** (1986) 1
- [7] S. Ambrosanio and B. Mele, Phys. Rev. **D 52** (1995) 3900; preprint Rome1-1095/95,
hep-ph/9508237

- [8] S.M. Barr, Phys. Lett. **B 112** (1982) 219
- [9] H.P. Nilles, M. Srednicki and D. Wyler, Phys. Lett. **B 120** (1983) 346
- [10] J.-P. Derendinger and C.A. Savoy, Nucl. Phys. **B 237** (1984) 307
- [11] M. Drees, Int. J. of Mod. Phys. **A4** (1989) 3635
- [12] J. Ellis, J.F. Gunion, H.E. Haber, L. Roszkowski and F. Zwirner, Phys. Rev. **D 39** (1989) 844
- [13] J.E. Kim and H.P. Nilles, Phys. Lett. **B 138** (1984) 150
- [14] S.A. Abel, S. Sarkar and P.L. White, preprint OUTP-95-22P, RAL-TR-95-019, hep-ph/9506359
- [15] F. Franke, H. Fraas and A. Bartl, Phys. Lett. **B 336** (1994) 415
- [16] F. Franke and H. Fraas, Phys. Lett. **B 353** (1995) 234
- [17] J.R. Espinosa and M. Quirós, Phys. Lett. **B 279** (1992) 92
- [18] U. Ellwanger, Phys. Lett. **B 303** (1993) 271;
T. Elliott, S.F. King and P.L. White, Phys. Lett. **B 314** (1993) 56;
P.N. Pandita, Phys. Lett. **B 318** (1993) 338; Z. Phys. **C 59** (1993) 575
- [19] U. Ellwanger, M. Rausch de Traubenberg, C.A. Savoy, Phys. Lett. **B 315** (1993) 331; Z. Phys. **C 67** (1995) 665
- [20] T. Elliott, S.F. King and P.L. White, Phys. Rev. **D 49** (1994) 2435
- [21] B.R. Kim, S.K. Oh and A. Stephan, Proceedings of the Workshop e^+e^- Collisions at 500 GeV. The Physics Potential, Munich, Annecy, Hamburg, Ed. by P. Zerwas, DESY 92-123B (1992) 697; DESY 93-123C (1993) 491; Proceedings of the Workshop on Physics and Experiments with Linear e^+e^- colliders, Vol. II, p. 860, World Scientific, Eds. F.A. Harris, S.L. Olsen, S. Pakvasa, X. Tata; Phys. Lett. **B 336** (1994) 200
- [22] S.F. King and P.L. White, preprint SHEP 95-27, OUTP-95-31P, hep-ph/9508346
- [23] K. Inoue, A. Kakuto, H. Komatsu and S. Takeshita, Prog. Theor. Phys. **67** (1982) 1889; **68** (1982) 927;
J.-P. Derendinger and C.A. Savoy, Nucl. Phys. **237** (1984) 307
- [24] K.A. Olive and D. Thomas, Nucl. Phys. **B 355** (1991) 192;
S.A. Abel, S. Sarkar and I.B. Whittingham, Nucl. Phys. **B 392** (1993) 83
- [25] P.N. Pandita, Phys. Rev. **D 50** (1994) 571
- [26] L.J. Hall and J. Polchinski, Phys. Lett. **B 152** (1985) 335
- [27] H.E. Haber and D. Wyler, Nucl. Phys. **B 323** (1989) 267

- [28] A. Bartl, H. Fraas, W. Majerotto and N. Oshimo, Phys. Rev. **D 40** (1989) 1594
- [29] F. Franke and H. Fraas, in preparation

Scenario A							
$M = 65 \text{ GeV}, x = 1000 \text{ GeV}, \lambda = 0.4, k = 0.001, \tan \beta = 2$							
		Mass [GeV]	Photino	Zino	Higgsino A	Higgsino B	Singlet
Neutralinos	$\tilde{\chi}_1^0$	-8	-.141	0.329	0.157	-.079	0.917
	$\tilde{\chi}_2^0$	-28	-.712	0.602	0.086	0.125	-.330
	$\tilde{\chi}_3^0$	-54	0.688	0.687	0.133	0.114	-.125
	$\tilde{\chi}_4^0$	412	-.002	0.061	0.314	-.934	-.157
	$\tilde{\chi}_5^0$	-423	0.008	0.231	-.923	-.303	0.050
Charginos			$m_{\tilde{\chi}_1^\pm} = -50 \text{ GeV}$			$m_{\tilde{\chi}_2^\pm} = 418 \text{ GeV}$	
Scenario B							
$M = 120 \text{ GeV}, x = 1000 \text{ GeV}, \lambda = 0.4, k = 0.001, \tan \beta = 2$							
		Mass [GeV]	Photino	Zino	Higgsino A	Higgsino B	Singlet
Neutralinos	$\tilde{\chi}_1^0$	-10	-.054	0.135	0.127	-.113	0.975
	$\tilde{\chi}_2^0$	-55	0.784	-.589	-.115	-.097	0.129
	$\tilde{\chi}_3^0$	-104	-.618	-.750	-.186	-.118	0.080
	$\tilde{\chi}_4^0$	412	-.003	0.055	0.313	-.935	-.157
	$\tilde{\chi}_5^0$	-425	0.019	0.264	-.915	-.230	0.049
Charginos			$m_{\tilde{\chi}_1^\pm} = -102 \text{ GeV}$			$m_{\tilde{\chi}_2^\pm} = 420 \text{ GeV}$	

Table 1: Scenarios A and B with a light singlet-like neutralino and different gaugino mass parameters M . Shown are the neutralino and chargino masses and the elements N_{ij} of the neutralino mixing matrix.

Scenario C							
$M = 200 \text{ GeV}, x = 1000 \text{ GeV}, \lambda = 0.4, k = 0.001, \tan \beta = 2$							
		Mass [GeV]	Photino	Zino	Higgsino A	Higgsino B	Singlet
Neutralinos	$\tilde{\chi}_1^0$	-11	0.026	-0.070	-0.116	0.123	0.983
	$\tilde{\chi}_2^0$	-94	0.812	-0.558	-0.132	-0.088	0.066
	$\tilde{\chi}_3^0$	-178	-0.581	-0.757	-0.261	0 - 133	0.053
	$\tilde{\chi}_4^0$	412	0.004	-0.049	-0.313	0.935	0.157
	$\tilde{\chi}_5^0$	-431	0.045	0.329	-0.896	-0.291	0.047
Charginos			$m_{\tilde{\chi}_1^\pm} = -176 \text{ GeV}$		$m_{\tilde{\chi}_2^\pm} = 427 \text{ GeV}$		
Scenario D							
$M = -120 \text{ GeV}, x = 1000 \text{ GeV}, \lambda = 0.4, k = 0.001, \tan \beta = 2$							
		Mass [GeV]	Photino	Zino	Higgsino A	Higgsino B	Singlet
Neutralinos	$\tilde{\chi}_1^0$	-12	0.022	-0.073	0.089	-0.142	0.983
	$\tilde{\chi}_2^0$	63	0.913	-0.396	-0.065	-0.047	-0.050
	$\tilde{\chi}_3^0$	130	-0.407	-0.900	-0.116	-0.123	-0.065
	$\tilde{\chi}_4^0$	413	-0.007	-0.095	-0.316	0.931	0.156
	$\tilde{\chi}_5^0$	-416	-0.008	0.164	-0.935	-0.310	0.052
Charginos			$m_{\tilde{\chi}_1^\pm} = 129 \text{ GeV}$		$m_{\tilde{\chi}_2^\pm} = 413 \text{ GeV}$		

Table 2: Scenarios C and D with a light singlet-like neutralino and gaugino mass parameters M with different signs. Shown are the neutralino and chargino masses and the elements N_{ij} of the neutralino mixing matrix.

Higgs bosons					
$x = 1000 \text{ GeV}, \lambda = 0.4, k = 0.001, \tan \beta = 2, A_t = 0 \text{ GeV}$					
$m_{\tilde{t}_1} = 150 \text{ GeV}, m_{\tilde{t}_2} = 500 \text{ GeV}$					
		Mass [GeV]	H_1^0	H_2^0	N
Scalars	S_1	37 – 54	0.001 – 0.114	0 – 0.318	0.941 – 0.999
	S_2	96 – 100	0.436 – 0.451	0.835 – 0.894	0.004 – 0.335
	S_3	972 – 1006	0.893	0.449	0.043
Pseudoscalars	P_1	7 – 51	0.062	0.031	0.998
	P_2	973 – 1006	0.892	0.446	0.069

Table 3: Higgs masses m_{S_a}, m_{P_α} and mixings $U_{ab}^S, U_{\alpha\beta}^P$, respectively, in the scenarios A – D.

Scenario E							
$M = 115 \text{ GeV}, x = 1000 \text{ GeV}, \lambda = 0.4, k = 0.035, \tan \beta = 2$							
		Mass [GeV]	Photino	Zino	Higgsino A	Higgsino B	Singlet
Neutralinos	$\tilde{\chi}_1^0$	-50	-.735	0.621	0.156	0.061	0.214
	$\tilde{\chi}_2^0$	-77	0.360	0.089	0.120	-.088	0.917
	$\tilde{\chi}_3^0$	-102	-.574	-.732	-.154	-.138	0.303
	$\tilde{\chi}_4^0$	411	-.003	0.056	0.315	-.938	-.136
	$\tilde{\chi}_5^0$	-425	0.018	0.260	-.916	-.301	0.059
Charginos			$m_{\tilde{\chi}_1^\pm} = -97 \text{ GeV}$	$m_{\tilde{\chi}_2^\pm} = 420 \text{ GeV}$			
Scenario F							
$M = -95 \text{ GeV}, x = 1000 \text{ GeV}, \lambda = 0.4, k = 0.035, \tan \beta = 2$							
		Mass [GeV]	Photino	Zino	Higgsino A	Higgsino B	Singlet
Neutralinos	$\tilde{\chi}_1^0$	50	0.922	-.379	-.062	-.048	-.028
	$\tilde{\chi}_2^0$	-78	0.008	-.054	0.094	-.116	0.988
	$\tilde{\chi}_3^0$	105	-.387	0.904	-.124	-.123	-.049
	$\tilde{\chi}_4^0$	412	-.005	-.089	-.318	0.934	0.135
	$\tilde{\chi}_5^0$	-416	0.008	-.170	0.933	0.310	-.062
Charginos			$m_{\tilde{\chi}_1^\pm} = 104 \text{ GeV}$	$m_{\tilde{\chi}_2^\pm} = 413 \text{ GeV}$			
Higgs bosons	$A_t = 0 \text{ GeV}, m_{\tilde{t}_1} = 150 \text{ GeV}, m_{\tilde{t}_2} = 500 \text{ GeV}$ $m_{S_1} = 43 - 86 \text{ GeV}, m_{S_2} = 96 - 119 \text{ GeV}, m_{S_3} = 930 - 1028 \text{ GeV}$ $m_{P_1} = 38 - 123 \text{ GeV}, m_{P_2} = 930 - 1029 \text{ GeV}$						

Table 4: Scenarios E and F with a singlet-like second lightest neutralino. Shown are the neutralino and chargino masses and the elements N_{ij} of the neutralino mixing matrix as well as the range of the Higgs masses.

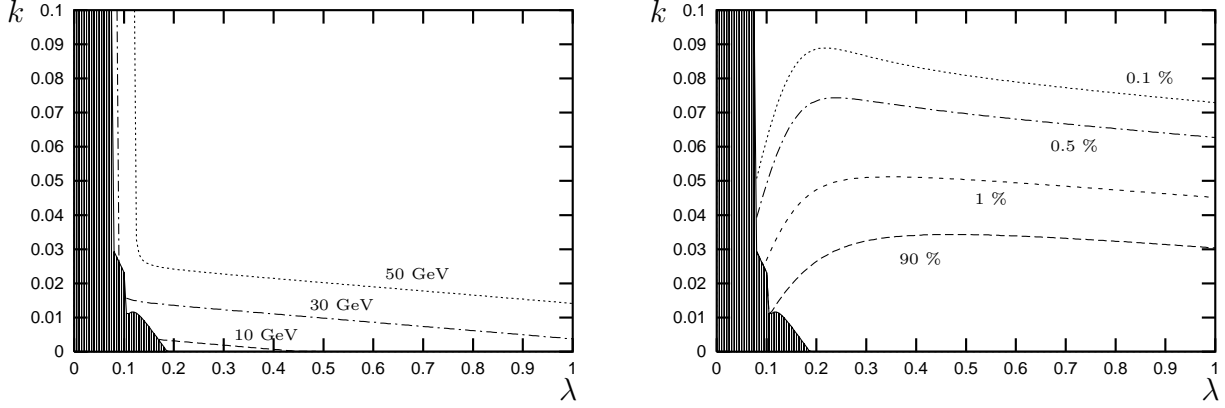
Scenario G							
$M = -90$ GeV, $x = 300$ GeV, $\lambda = 0.4$, $k = 0.1$, $\tan \beta = 2$							
		Mass [GeV]	Photino	Zino	Higgsino A	Higgsino B	Singlet
Neutralinos	$\tilde{\chi}_1^0$	50	0.953	-.258	-.115	-.092	-.058
	$\tilde{\chi}_2^0$	-79	0.022	-.154	0.264	-.256	0.917
	$\tilde{\chi}_3^0$	105	-.286	-.750	-.150	-.532	-.224
	$\tilde{\chi}_4^0$	156	-.091	0.485	0.387	-.741	-.238
	$\tilde{\chi}_5^0$	-157	-.030	0.335	-.863	-.306	0.220
Charginos	$m_{\tilde{\chi}_1^\pm} = 100$ GeV		$m_{\tilde{\chi}_2^\pm} = 159$ GeV				
Higgs bosons	$A_t = 0$ GeV, $m_{\tilde{t}_1} = 150$ GeV, $m_{\tilde{t}_2} = 500$ GeV						
	$m_{S_1} = 7 - 73$ GeV, $m_{S_2} = 91 - 107$ GeV, $m_{S_3} = 252 - 326$ GeV						
	$m_{P_1} = 60 - 136$ GeV, $m_{P_2} = 245 - 323$ GeV						

Table 5: Scenario G with a smaller singlet vacuum expectation value x and a singlet-like second lightest neutralino. Shown are the neutralino and chargino masses and the elements N_{ij} of the neutralino mixing matrix as well as the range of the Higgs masses.

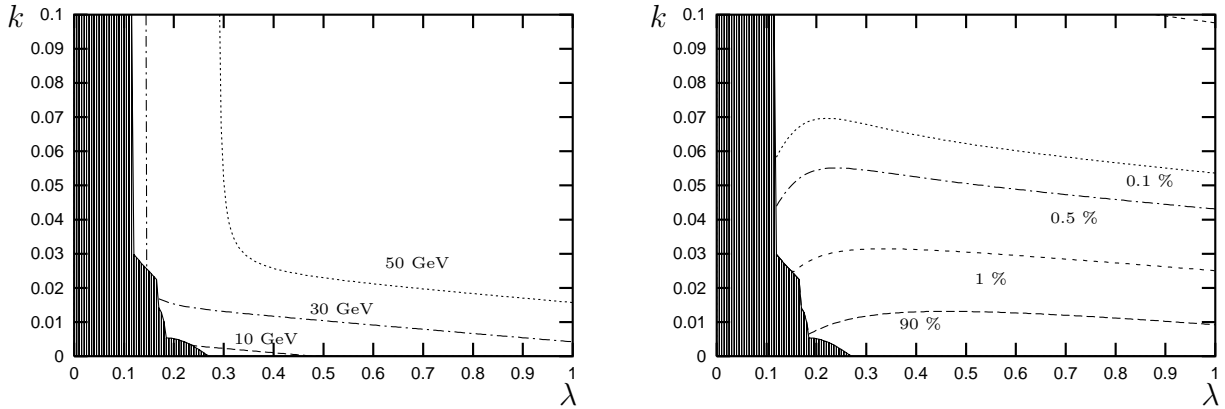
	Scenario E		Scenario F		Scenario G	
	$A_\lambda = 900 \text{ GeV}$ $A_k = 50 \text{ GeV}$		$A_\lambda = 900 \text{ GeV}$ $A_k = 50 \text{ GeV}$		$A_\lambda = 250 \text{ GeV}$ $A_k = 30 \text{ GeV}$	
	$A_t = 0 \text{ GeV}, m_{\tilde{t}_1} = 150 \text{ GeV}, m_{\tilde{t}_2} = 500 \text{ GeV}$					
	Γ/GeV	BR	Γ/GeV	BR	Γ/GeV	BR
$\tilde{\chi}_2^0 \rightarrow \tilde{\chi}_1^0 e^+ e^-$	$8.60 \cdot 10^{-9}$	0.55	$9.60 \cdot 10^{-11}$	0.07	$1.29 \cdot 10^{-9}$	0.14
$\tilde{\chi}_2^0 \rightarrow \tilde{\chi}_1^0 \nu \bar{\nu}$	$1.82 \cdot 10^{-9}$	0.12	$1.47 \cdot 10^{-11}$	0.01	$7.25 \cdot 10^{-10}$	0.08
$\tilde{\chi}_2^0 \rightarrow \tilde{\chi}_1^0 q \bar{q}$	$3.23 \cdot 10^{-9}$	0.21	$3.23 \cdot 10^{-10}$	0.22	$5.80 \cdot 10^{-9}$	0.61
$\tilde{\chi}_2^0 \rightarrow \tilde{\chi}_1^0 \gamma$	$1.83 \cdot 10^{-9}$	0.12	$1.00 \cdot 10^{-9}$	0.70	$1.60 \cdot 10^{-9}$	0.17
$\tilde{\chi}_3^0 \rightarrow \tilde{\chi}_1^0 e^+ e^-$	$9.95 \cdot 10^{-8}$	0.10	$5.21 \cdot 10^{-7}$	0.39	$3.14 \cdot 10^{-7}$	0.10
$\tilde{\chi}_3^0 \rightarrow \tilde{\chi}_1^0 \nu \bar{\nu}$	$2.69 \cdot 10^{-7}$	0.26	$2.19 \cdot 10^{-7}$	0.17	$1.05 \cdot 10^{-7}$	0.03
$\tilde{\chi}_3^0 \rightarrow \tilde{\chi}_1^0 q \bar{q}$	$5.86 \cdot 10^{-7}$	0.57	$5.48 \cdot 10^{-7}$	0.41	$2.75 \cdot 10^{-6}$	0.86
$\tilde{\chi}_3^0 \rightarrow \tilde{\chi}_1^0 \gamma$	$6.06 \cdot 10^{-9}$	0.006	$9.88 \cdot 10^{-9}$	0.007	$2.16 \cdot 10^{-8}$	0.007
$\tilde{\chi}_3^0 \rightarrow \tilde{\chi}_1^\pm e^\mp \nu$	$1.64 \cdot 10^{-9}$	0.001	$7.08 \cdot 10^{-13}$	< 0.001	$2.47 \cdot 10^{-9}$	< 0.001
$\tilde{\chi}_3^0 \rightarrow \tilde{\chi}_1^\pm q q'$	$4.92 \cdot 10^{-9}$	0.005	$2.12 \cdot 10^{-12}$	< 0.001	$7.39 \cdot 10^{-9}$	< 0.001
$\tilde{\chi}_3^0 \rightarrow \tilde{\chi}_2^0 e^+ e^-$	$7.24 \cdot 10^{-9}$	0.007	$2.16 \cdot 10^{-10}$	< 0.001	$4.38 \cdot 10^{-10}$	< 0.001
$\tilde{\chi}_3^0 \rightarrow \tilde{\chi}_2^0 \nu \bar{\nu}$	$1.62 \cdot 10^{-9}$	0.001	$2.08 \cdot 10^{-11}$	< 0.001	$2.48 \cdot 10^{-11}$	< 0.001
$\tilde{\chi}_3^0 \rightarrow \tilde{\chi}_2^0 q \bar{q}$	$2.24 \cdot 10^{-8}$	0.02	$1.54 \cdot 10^{-9}$	0.001	$3.41 \cdot 10^{-9}$	< 0.001
$\tilde{\chi}_3^0 \rightarrow \tilde{\chi}_2^0 \gamma$	$2.59 \cdot 10^{-8}$	0.02	$2.75 \cdot 10^{-8}$	0.02	$2.16 \cdot 10^{-8}$	0.007

Table 6: Decay widths and branching ratios for the decays of the second and third neutralinos in the scenarios E – G.

$M = 200 \text{ GeV}, x = 1000 \text{ GeV}, \tan \beta = 2$



$M = 120 \text{ GeV}, x = 1000 \text{ GeV}, \tan \beta = 2$



$M = 65 \text{ GeV}, x = 1000 \text{ GeV}, \tan \beta = 2$

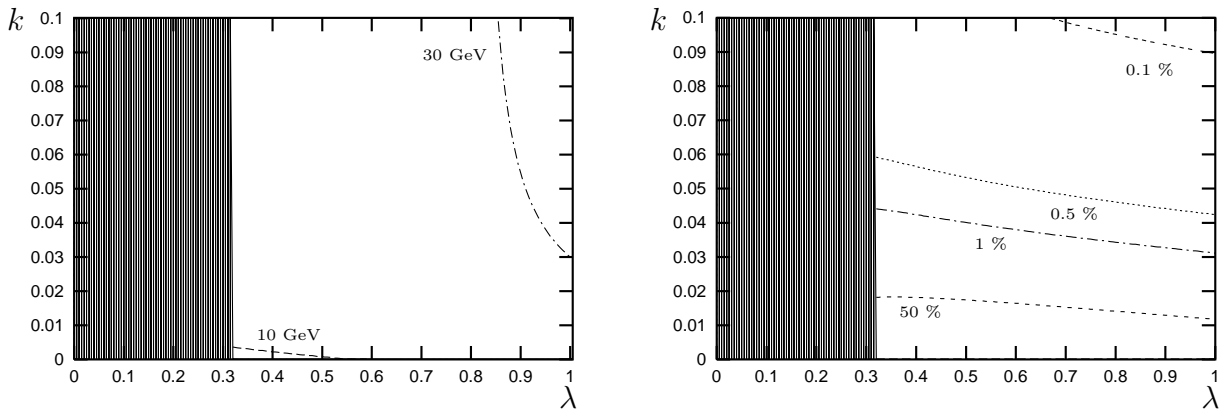


Figure 1: Contour lines of the mass $m_{\tilde{\chi}_1^0}$ and singlet component $|\langle \psi_N | \chi_1^0 \rangle|^2$ of the lightest neutralino in the (λ, k) -plane. The experimentally excluded domain is shaded.

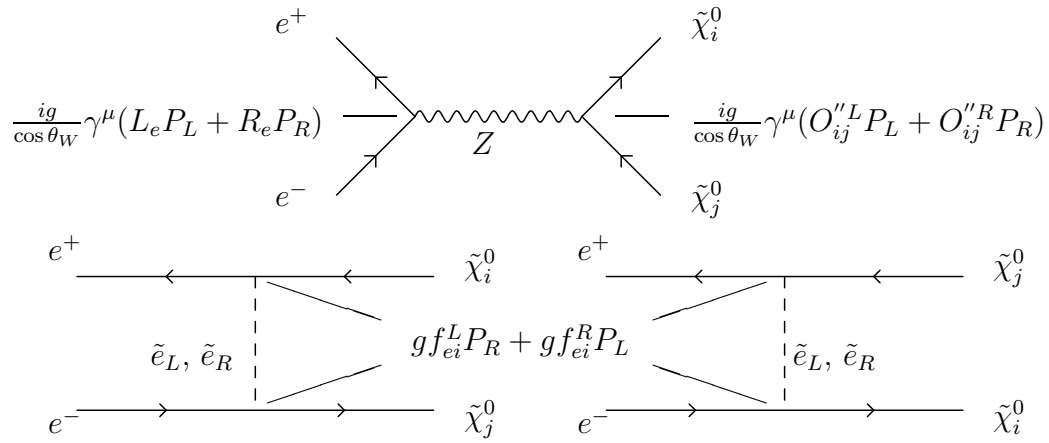


Figure 2: Feynman graphs and vertex factors for the process $e^+e^- \rightarrow \tilde{\chi}_i^0\tilde{\chi}_j^0$ ($i, j = 1, \dots, 5$). Explicit expressions for the parameters $L_e, R_e, f_{ei}^L, f_{ei}^R, O_{ij}^{\prime\prime L}, O_{ij}^{\prime\prime R}$ are given in the appendix.

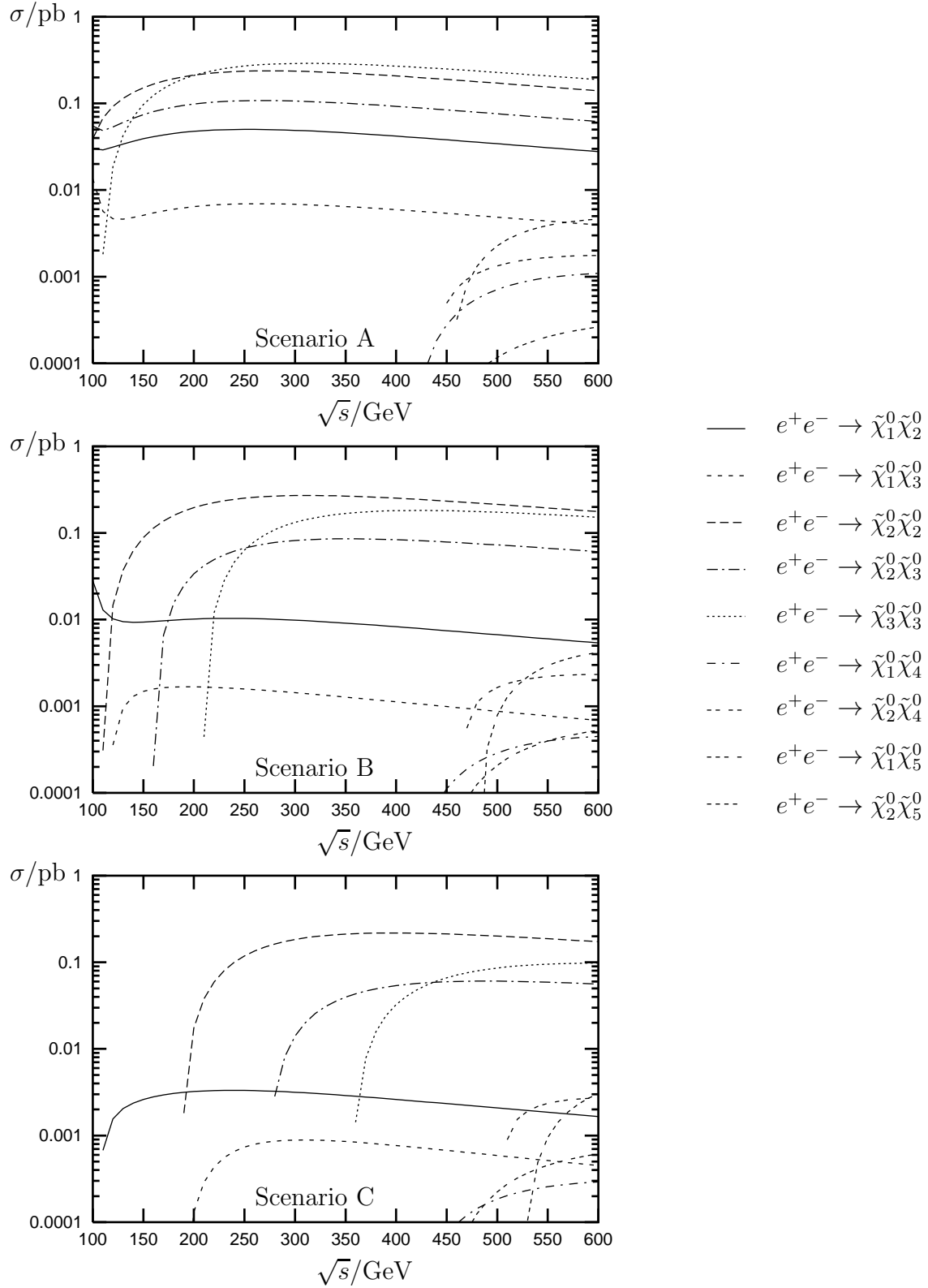


Figure 3: Cross sections for $e^+e^- \rightarrow \tilde{\chi}_i^0 \tilde{\chi}_j^0$ in scenarios A – C.

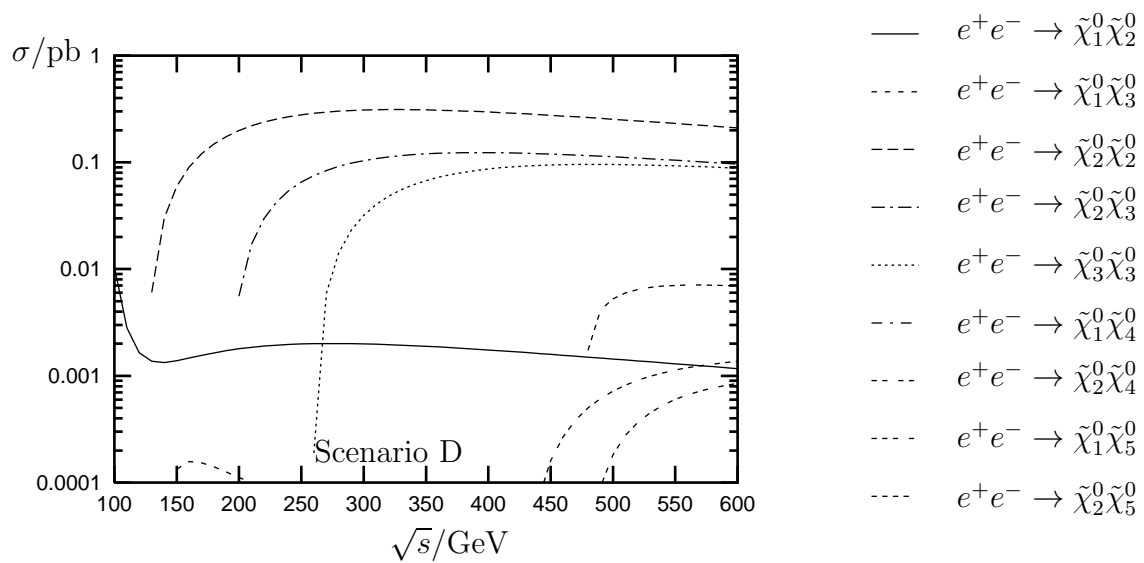


Figure 4: Cross sections for $e^+e^- \rightarrow \tilde{\chi}_i^0 \tilde{\chi}_j^0$ in scenario D.

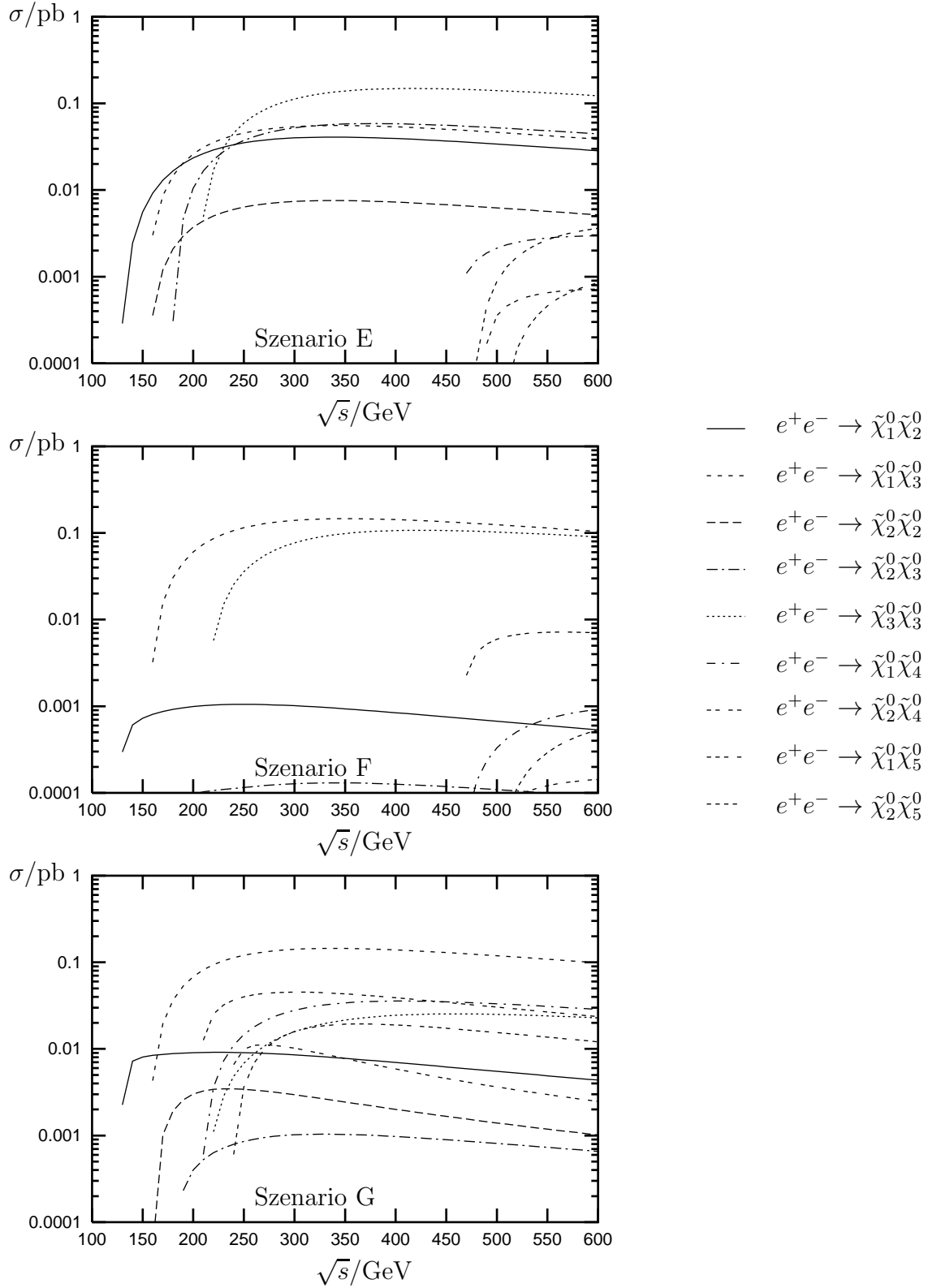


Figure 5: Cross sections for $e^+e^- \rightarrow \tilde{\chi}_i^0\tilde{\chi}_j^0$ in the scenarios E – G.

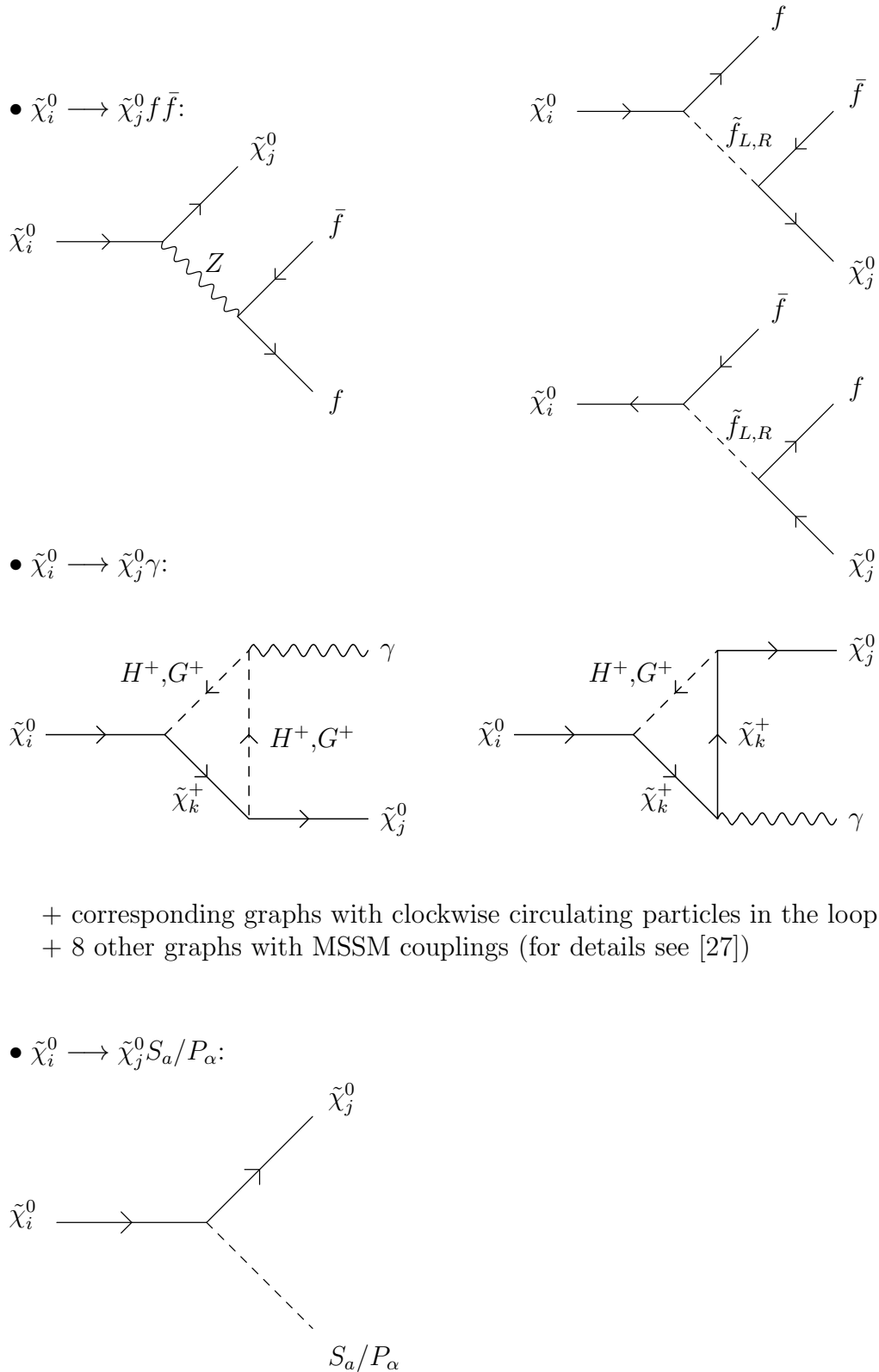


Figure 6: Feynman graphs for the considered neutralino decays.

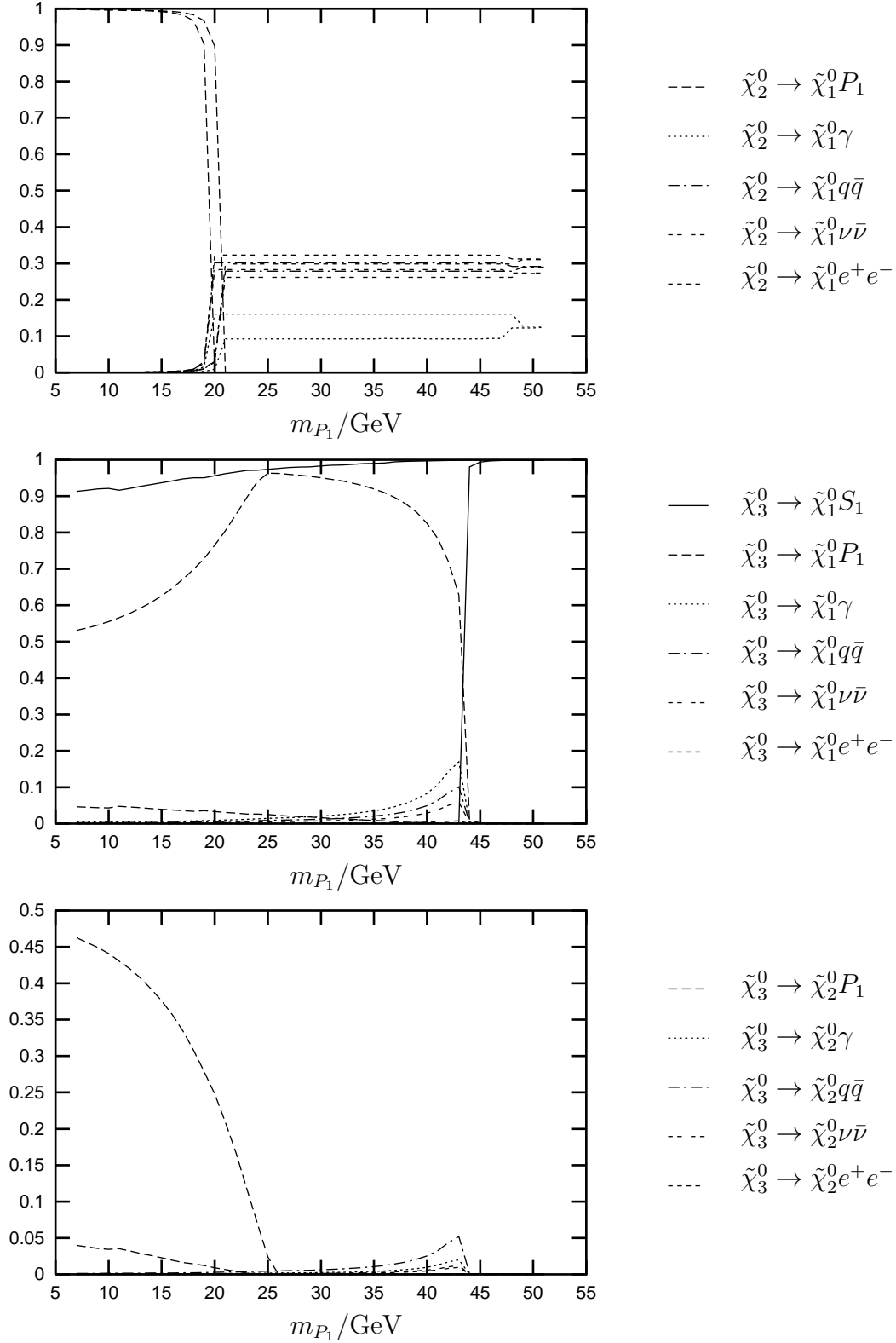


Figure 7: Minima und maxima of the branching ratios of the neutralino decays in scenario A as a function of the mass of the light pseudoscalar Higgs boson.

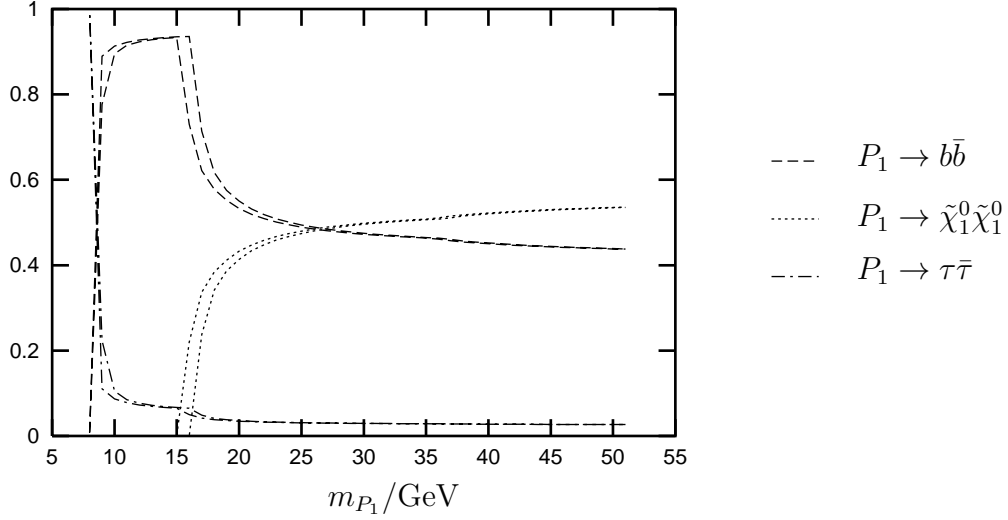


Figure 8: Minima und Maxima of the branching ratios of the decays of the light pseudo-scalar Higgs boson in scenario A.

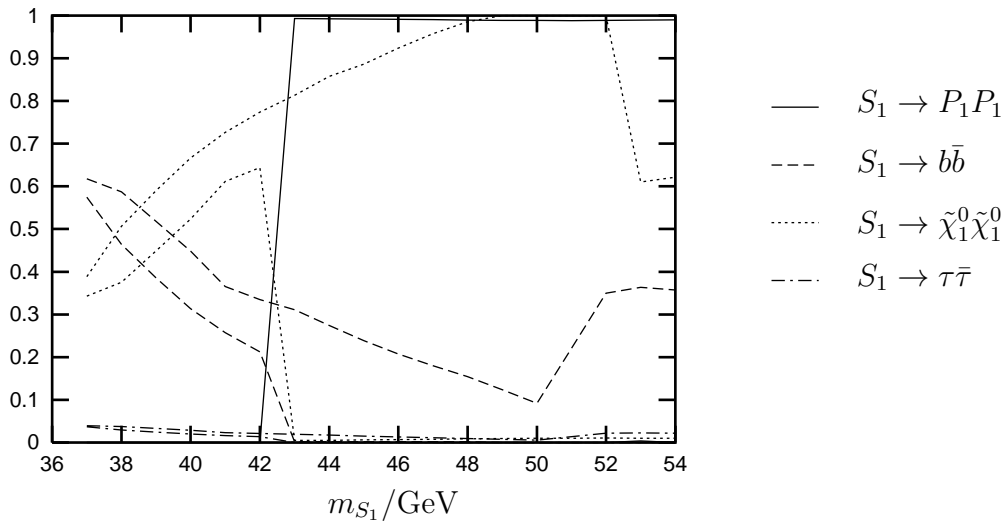


Figure 9: Minima und Maxima of the branching ratios of the decays of the lightest scalar Higgs boson in scenario A.

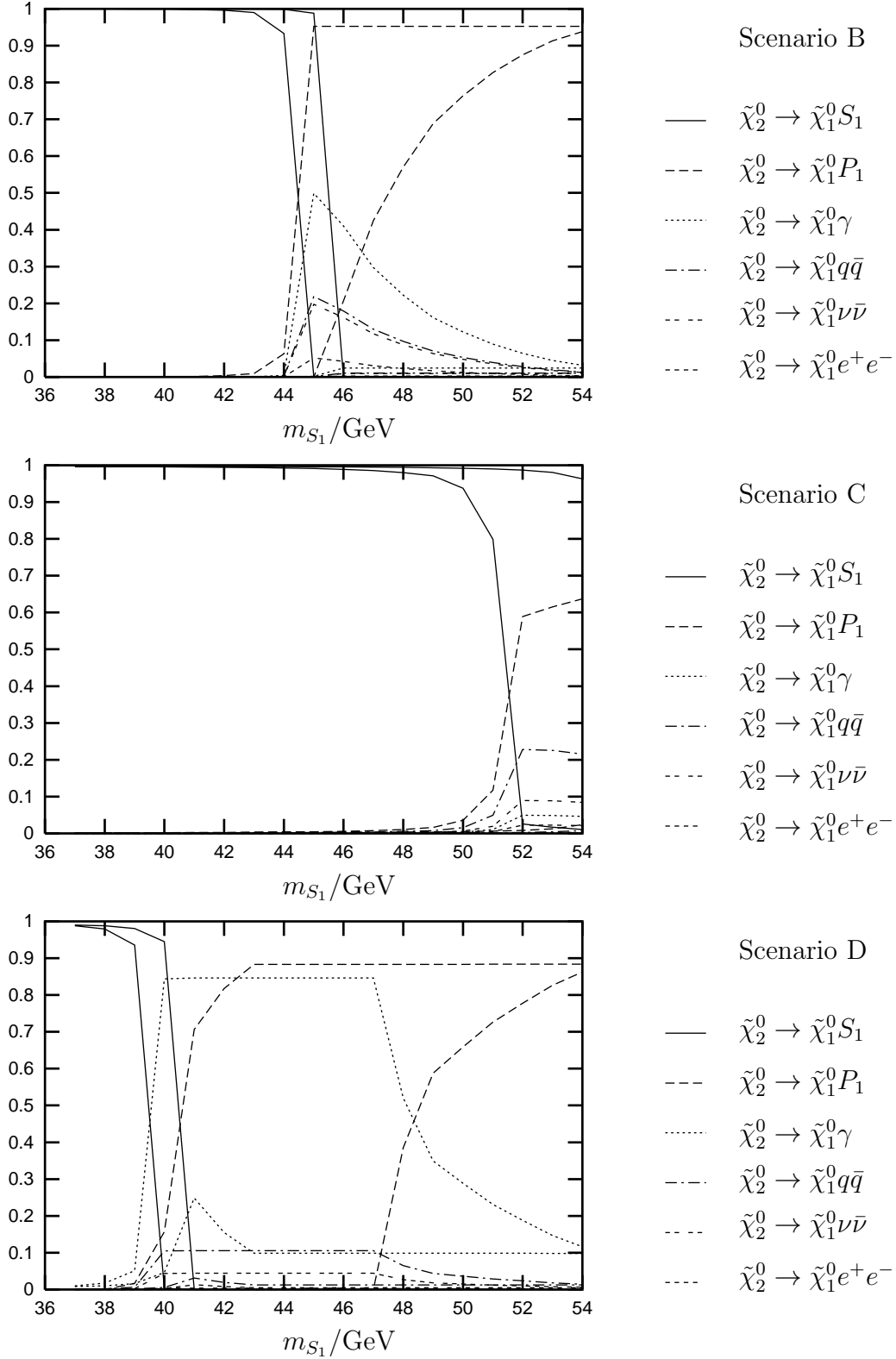


Figure 10: Minima und maxima of the branching ratios of the neutralino decays in scenarios B – D as a function of the mass of the lightest scalar Higgs boson.